Title

ON MACROSCOPIC AND MICROSCOPIC ANALYSES FOR CRACK INITIATION AND CRACK GROWTH TOUGHNESS IN DUCTILE ALLOYS

Authors

Ritchie, R.O.
Thompson, A.W.

Publication Date

1983-12-01

Lawrence Berkeley Laboratory

UNIVERSITY OF CALIFORNIA

Materials & Molecular Research Division

Submitted to Metallurgical Transactions A

ON MACROSCOPIC AND MICROSCOPIC ANALYSES FOR CRACK INITIATION AND CRACK GROWTH TOUGHNESS IN DUCTILE ALLOYS

R.O. Ritchie and A.W. Thompson

December 1983

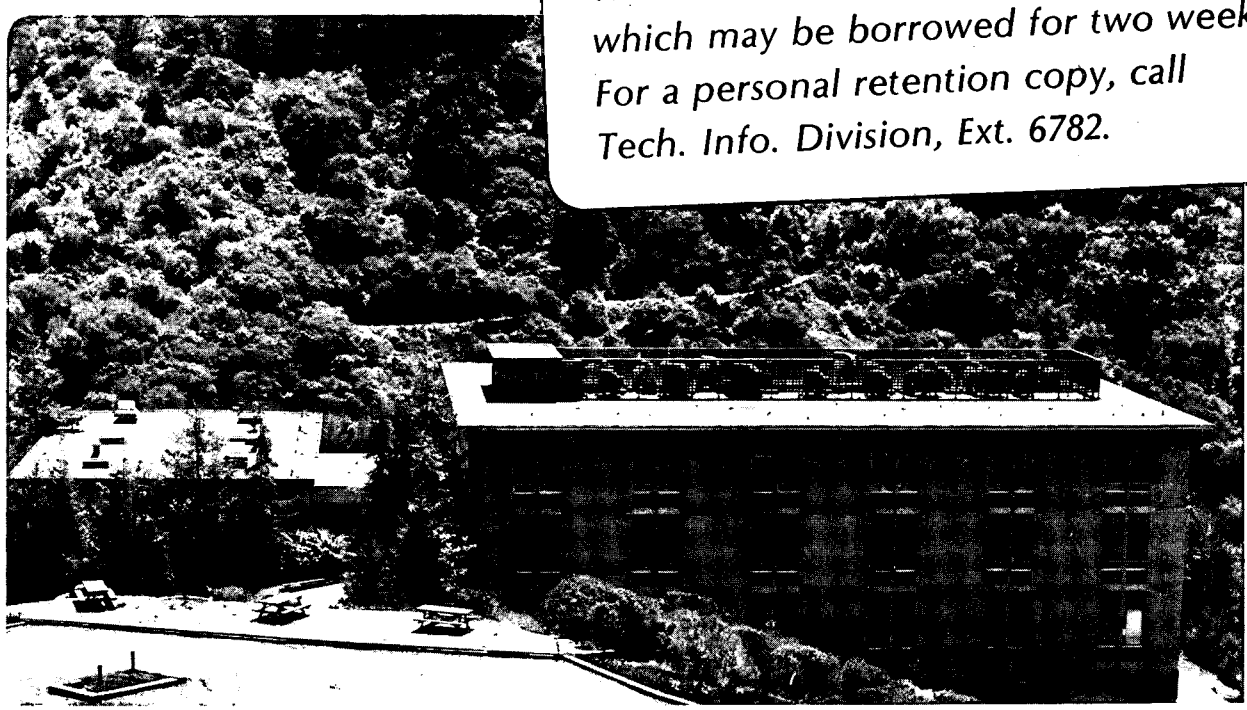

Prepared for the U.S. Department of Energy under Contract DE-AC03-76SF00098

DISCLAIMER

LBL-16603

ON MACROSCOPIC AND MICROSCOPIC ANALYSES FOR CRACK INITIATION AND CRACK GROWTH TOUGHNESS IN DUCTILE ALLOYS

by

R. O. Ritchie

Materials and Molecular Research Division, Lawrence Berkeley Laboratory,
and Department of Materials Science and Mineral Engineering,
University of California, Berkeley, CA 94720

and

A. W. Thompson

Department of Metallurgical Engineering and Materials Science,
Carnegie-Mellon University, Pittsburgh, PA 15213

December 1983

submitted to Metallurgical Transactions A

This work was supported by the Director, Office of Energy Research, Office of Basic Energy Sciences, Materials Science Division of the U.S. Department of Energy under Contract No. DE-AC03-76SF00098, and by the U.S. National Science Foundation under Grant No. 81-19541.

ON MACROSCOPIC AND MICROSCOPIC ANALYSES FOR CRACK INITIATION AND CRACK GROWTH TOUGHNESS IN DUCTILE ALLOYS

R. O. Ritchie and A. W. Thompson

ABSTRACT

Relationships between crack initiation and crack growth toughness are reviewed by examining the crack tip fields and microscopic (local) and macroscopic (continuum) fracture criteria for the onset and continued quasi-static extension of cracks in ductile materials. By comparison of the micromechanisms of crack initiation via transgranular cleavage and crack initiation and subsequent growth via microvoid coalescence, expressions are shown for the fracture toughness of materials in terms of microstructural parameters, including those deduced from fractographic measurements. In particular the distinction between the deformation fields directly ahead of stationary and non-stationary cracks are explored and used to explain why microstructure may have a more significant role in influencing the toughness of slowly growing, as opposed to initiating, cracks. Utilizing the exact asymptotic crack tip deformation fields recently presented by Rice and his co-workers for the non-stationary plane strain Mode I crack and evoking various microscopic failure criteria for such stable crack

---

R. O. RITCHIE is Professor in the Materials and Molecular Research Division, Lawrence Berkeley Laboratory, and Department of Materials Science and Mineral Engineering, University of California, Berkeley, CA 94720. A. W. THOMPSON is Professor in the Department of Metallurgical Engineering and Materials Science, Carnegie-Mellon University, Pittsburgh, PA 15213.

growth, a relationship between the tearing modulus T_R and the non-dimensionalized crack initiation fracture toughness J_{IC} is described and shown to yield a good fit to experimental toughness data for a wide range of steels.

I. INTRODUCTION

The fracture toughness of a material is conventionally assessed in terms of the critical value of some crack tip field characterizing parameter at the **initiation** of unstable crack growth. In plane strain for example, under small-scale yielding (ssy) conditions, the critical value of the linear elastic stress intensity factor, K_{Ic}, is generally determined at the onset of crack extension, and can be referred to as the "toughness."[1] With appreciable non-linearity in the load-displacement curve, however, the (crack initiation) toughness is measured in terms of the critical value of the J-integral, J_{Ic},[2,3] or the crack tip opening displacement, δ_i or δ_{Ic}.[4] For ssy conditions, these parameters are explicitly related in terms of the flow stress, σ_o, and the elastic (Young's) modulus E, i.e.:

$$J_{Ic} = \frac{K_{Ic}^2}{E'} = \frac{1}{\alpha}\delta_i\sigma_o \quad , \qquad (1)$$

where $E' = E$ in plane stress and $E/(1-\nu^2)$ in plane strain, and α is a proportionality factor of order unity, dependent upon the yield strain ($\varepsilon_o = \sigma_o/E$), the work hardening exponent (n) and whether plane stress or plane strain conditions are assumed.[5]

Although in "brittle" structures, catastrophic failure or instability is effectively coincident with this onset of crack extension, in the presence of sufficient crack tip plasticity, crack initiation is generally followed by a region of stable crack growth.

Under elastic-plastic conditions (or plane stress, linear elastic conditions), such sub-critical crack advance has been macroscopically characterized in terms of crack growth resistance curves, i.e., the $J_R(\Delta a)$ and $\delta_R(\Delta a)$ R curves (Fig. 1).[6-8] Crack **growth** toughness is now assessed in terms of the slope of the resistance curve, which in the J approach can be evaluated in terms of the non-dimensional tearing modulus ($T_R = \frac{E}{\sigma_o^2} \cdot \frac{dJ}{da}$),[7] or in the CTOD approach in terms of the crack tip opening angle (CTOA $= \frac{d\delta}{da}$),[8,9] where:

$$T_R \equiv \frac{E}{\sigma_o^2}\frac{dJ}{da} = \frac{E}{\sigma_o}\frac{d\delta}{da} = \frac{\text{CTOA}}{\text{Yield Strain}} \quad . \qquad (2)$$

Whereas crack initiation toughness values (i.e., K_{Ic}, J_{Ic}, etc.) are by far the most widely measured and quoted, it has been noted in high toughness ductile materials, for example, that stable ductile crack growth can occur at J values some 5 to 10 or more times the initial J_{Ic} value prior to instability,[10] e.g., Fig. 2. Furthermore, microstructural influences on fracture resistance would appear to be enhanced in the crack growth regime, compared to initiation behavior (Fig. 2). Evaluating the toughness of such materials with crack **initiation** parameters, such as J_{Ic}, would appear overly conservative, and accordingly there has been a recent trend, both for engineering fracture mechanics design and for metallurgical toughness assessment, to consider additionally crack **growth** parameters, such as dJ/da, CTOA or the tearing modulus T_R (for reviews, see refs. 6-12).

The purpose of this paper is to examine the relationship between crack initiation and quasi-static crack growth toughness at both macroscopic and microscopic levels and in particular to identify the role of microstructure. Continuum and local models for the initiation and continued propagation of cracks, by both cleavage and hole growth mechanisms, are considered in terms of near-tip stress and deformation fields and macroscopic/microscopic fracture criteria for the quasi-static plane strain advance of stationary and non-stationary tensile cracks. Specifically, model expressions for crack initiation and crack growth toughness are presented which indicate a relationship between J_{Ic} and T_R, the latter representing an extension of the brief assessment of crack growth toughness originally reported by Shih et al.[13]

II. CRACK INITIATION TOUGHNESS

Crack Tip Fields for Stationary Cracks

The stress and deformation fields local to the near-tip region of stationary cracks subjected to tensile (Mode I) opening are well known for both linear elastic and non-linear elastic solids. Asymptotic continuum mechanics analyses of the local singular fields yield, for linear elastic conditions, a local stress distribution at distance r from the crack tip, in the limit of $r \to 0$, of:[14,15]

$$\sigma_{ij}(r,\theta) \to \frac{K_I}{\sqrt{2\pi r}} f_{ij}(\theta) \quad , \tag{3}$$

where K_I is the Mode I stress intensity factor, θ the polar angle measured from the crack plane, and f_{ij} a dimensionless function of θ. For elastic-plastic (actually non-linear elastic) conditions, asymptotic solutions by Hutchinson, Rice and Rosengren (HRR) for the local stress, strain and displacements ahead of a stationary tensile crack in a power-hardening (incompressible non-linear elastic) solid, with a constitutive relationship of the form:

$$\bar{\sigma} = \bar{\sigma}_1 (\bar{\varepsilon}_p)^n \quad , \tag{4}$$

yield, in the limit of $r \to 0$:[16,17]

$$\frac{\sigma_{ij}(r,\theta)}{\bar{\sigma}_1} \to \left(\frac{J}{\bar{\sigma}_1 I_n r}\right)^{\frac{n}{n+1}} \tilde{\sigma}_{ij}(\theta) \quad , \tag{5a}$$

$$\varepsilon^p_{ij}(r,\theta) \rightarrow \left(\frac{J}{\bar{\sigma}_1 I_n r}\right)^{\frac{1}{n+1}} \tilde{\varepsilon}^p_{ij}(\theta) \quad , \tag{5b}$$

$$\frac{u_i(r,\theta)}{r} \rightarrow \left(\frac{J}{\bar{\sigma}_1 I_n r}\right)^{\frac{1}{n+1}} \tilde{u}_i(\theta) \quad , \tag{5c}$$

where J is the J-integral,[18] $\bar{\sigma}_1$ the equivalent stress at unit strain, $\tilde{\sigma}_{ij}(\theta)$, $\tilde{\varepsilon}_{ij}(\theta)$ and $\tilde{u}_i(\theta)$ are normalized stress, strain and displacement functions of θ, and I_n is a numerical constant, weakly dependent upon the strain hardening exponent, n, given within 2 pct by the empirical relation:[19,20]

$$I_n = 10.3\sqrt{0.13 + n} - 4.8\, n \quad . \tag{6}$$

Numerical values of the functions in Eq. 5 have recently been tabulated by Shih.[21]

Incorporating Rice and Johnson's[22] and McMeeking's[23] near-tip blunting solutions which consider large geometry changes at the crack tip, and Tracey's[24] numerical power hardening solutions, the distribution of local tensile (opening) stress, σ_{yy}, directly ahead of a **stationary** Mode I crack (i.e., at $\theta = 0$ when $r = x$) can be defined for various values of n and σ_o/E, as shown in Fig. 3. The corresponding near-tip equivalent plastic strain ($\bar{\varepsilon}_p$) distribution,[22] which is essentially independent of strain hardening for the stationary crack,[23] is shown in Fig. 4. Also plotted is the near-tip variation of

stress state, defined as the ratio of hydrostatic to equivalent stress ($\sigma_m/\bar{\sigma}$).

Continuum (Macroscopic) Fracture Initiation Criteria

To define macroscopic fracture criteria for crack initiation, reference is made to the functional form of the local singular fields from the continuum asymptotic analyses (Eqs. 3 and 5). For a brittle solid, the stress intensity factor K_I can be considered as the (scalar) amplitude of the linear elastic singularity in Eq. (3). Under conditions of small-scale yielding (ssy), where the plastic zone size (r_y) at the crack tip, given approximately by:[15]

$$r_y \approx \frac{1}{2\pi} \left(\frac{K_I}{\sigma_o}\right)^2 , \qquad (7)$$

is small compared to the length of the crack (a) and uncracked ligament (b), provided this asymptotic field "dominates" the local crack tip vicinity over dimensions large compared to the scale of microstructural deformation and fracture events involved, K_I can be utilized as a single, configuration-independent parameter which uniquely and autonomously characterizes the local stress and strain field ahead of a linear elastic crack. In such circumstances it can thus be utilized to correlate microscopically with crack extension. For the monotonic loading of plane strain stationary cracks, the onset of brittle fracture is thus macroscopically defined at $K_I = K_{Ic}$, where K_{Ic} is the Mode I plane strain fracture toughness.[1,15]

In the presence of more extensive plasticity where ssy conditions no longer apply (i.e., typically for $r_y \nless \frac{1}{15}$ (a,b)), J, taken as the scalar amplitude factor of the HRR singularity (Eq. 5), can be utilized in somewhat analogous fashion. Provided this field can be considered to dominate over the relevant crack tip dimensions, J uniquely and autonomously characterizes the local stresses and strains ahead of a stationary crack in a power hardening solid, and the corresponding macroscopic failure criterion for the onset of crack extension in a ductile solid becomes $J = J_{Ic}$.[2,3]

It should be noted here that the HRR singularity and the J-integral are strictly defined for a non-linear elastic solid, where stress is proportional to current strain, rather than for the more realistic elastic-incrementally plastic solid, where stress is proportional to strain increment (Fig. 5). Provided the crack remains stationary and is subjected only to a monotonically increasing load, plastic loading will not depart radically from proportionality and this approach is appropriate. However, for growing cracks where regions of elastic unloading and nonproportional plastic flow will be embedded in the J-dominated field, behavior is not properly modelled by non-linear elasticity, and this poses certain restrictions to the J characterization for large-scale yielding (c.f., ref. 12). Moreover, the uniqueness of the crack tip fields implied by the HRR singularity is only relevant in the presence of some strain hardening, since the crack tip fields for rigid/perfectly plastic bodies under full yielding conditions are very dependent on geometry. As noted by McClintock,[25]

the plane strain slip-line field for a fully yielded edge-cracked plate in bending (essentially the Prandtl field) has a fundamentally different near-tip stress and strain field compared to the center cracked plate in tension (Fig. 6). The former Prandtl field develops high triaxiality and normal stress ahead of the tip, with r^{-1} singular shear strains in the fan above and below, whereas in the latter case only modest triaxiality occurs ahead of the tip, but intense shear strains develop on planes at 45 deg. to the crack. Rationalizing such nonunique fully plastic solutions with the concept of a unique HRR field and J_{Ic} being a single valued configuration-independent measurement of toughness requires that some strain hardening must exist. This implies that, unlike K_I characterization, the specimen size limitations for single parameter J characterization must depend upon geometry. Finite strain, finite element calculations by McMeeking and Parks[26] suggest that these critical size limitations, in terms of the uncracked ligament dimension b, vary from

$$b > 25\ J/\sigma_o \quad , \text{ for the edge-cracked bend specimen} \qquad (8)$$

to

$$b > 200\ J/\sigma_o \quad , \text{ for the center-cracked tension specimen} \qquad (9)$$

for materials of moderately low strain hardening (n = 0.1), where σ_o

is the flow stress, usually defined as the mean of the yield and ultimate tensile strengths.

Local (Microscopic) Fracture Initiation Criteria

Since both macroscopic criteria, based on K_I or J, result from the asymptotic continuum mechanics characterization, realistic evaluation of toughness using K_{Ic} or J_{Ic} does not necessitate any microscopic understanding of the fracture events involved. However, in the interest of a full comprehension of a fracture process and specifically to define which microstructural features contribute to a material's toughness, it is often beneficial to construct microscopic models for specific fracture mechanisms. Such models are generally referred to as "micromechanisms". Unlike the continuum approach, this requires a microscopic model for the particular fracture mode, which incorporates a local failure criterion and consideration of salient microstructural features, as well as detailed knowledge of both the asymptotic and very-near tip stress and deformation fields. Physical fracture processes, and consequently the local failure criterion and characteristic microstructural dimensions, vary substantially, however, with fracture mode, as Fig. 7 illustrates for the four classical fracture morphologies, i.e., microvoid coalescence, quasi-cleavage, intergranular, and transgranular cleavage.

In view of the specificity of such models to particular fracture mechanisms for particular microstructures, a complete microscopic/macroscopic characterization of toughness has only been

achieved in a few simplified cases. For example, for slip-initiated transgranular cleavage fracture (Fig. 7d) in ferritic steels, Ritchie, Knott and Rice (RKR)[27] have shown that the onset of brittle crack extension at $K_I = K_{Ic}$ is consistent with a critical stress model in which the local tensile opening stress (σ_{yy}) directly ahead of the crack must exceed a local fracture stress (σ_f^*)† over a **microstructurally significant characteristic distance** ($x = \ell_o^*$), as depicted in Fig. 8a. Using the HRR field in Eq. (5) to define the crack tip stress field, the RKR model for the cleavage fracture toughness implies:[27-29]

$$K_{Ic} \propto [(\sigma_f^*)^{\frac{1+n}{2}} / (\sigma_o)^{\frac{1-n}{2}}] \ell_o^{*\frac{1}{2}} , \qquad (10)$$

where the proportionality factor is simply a function of I_n in the HRR solution, which can be inferred from tabulations in ref. 21.

In mild steels, with ferrite/carbide microstructures, the characteristic distance was found to be on the order of the spacing of the void initiating grain boundary carbides, i.e., typically $\sim$ two grain diameters (d_g),[27] although different size scales have been found when the analysis is applied to other materials.†† The model has been

†Extensive studies on cleavage fracture in mild steels indicate that σ_f^* is essentially independent of temperature below the ductile/brittle transition (see ref. 4).

††In addition, recent modelling studies by Evans[30] of cleavage in mild steel, using weakest link statistical considerations of the size distribution of cracked carbides, have interpreted the characteristic distance as the carbide location with the highest elemental failure probability pertinent to crack advance.

found to be particularly successful both in quantitatively predicting cleavage fracture toughness values in a wide range of microstructures and furthermore in rationalizing the influence on K_{Ic} of such variables as temperature,[27,29,31] strain rate,[29,31,32] neutron irradiation,[29,32] warm pre-stressing,[33] and so forth. Somewhat similar microscopic models involving a critical stress criterion have been suggested for other fracture modes, including intergranular cracking (Fig. 7c) in temper embrittled steels[34,35] and hydrogen-assisted fracture.[36]

For initiation of ductile fracture by microvoid coalescence (Fig. 7a), McClintock,[9] Rice and Johnson[22] and Rice and Tracey[37] considered the criterion that the critical crack tip opening displacement must exceed half the mean void-initiating particle spacing (i.e., $2\delta \approx \ell_o^* \sim d_p$), based on the notion that, in non-hardening materials, this would take place when the void sites are first enveloped by the intense strain region at the crack tip (i.e., at distance $x \sim 2\delta$ from the tip). This model implies that:

$$\delta_i = \delta_{Ic} \approx (0.5 \text{ to } 2)\, d_p \quad , \tag{11a}$$

or

$$J_{Ic} \sim \sigma_o \ell_o^* \quad , \tag{11b}$$

although it is unusual to find the fracture toughness to increase directly with increasing strength.

This problem is overcome by the approach of McClintock,[38] Mackenzie et al.[39] and others[29,40] who have alternatively utilized a stress-

modified critical strain criterion. Here, at $J = J_{Ic}$, the local equivalent plastic strain $\bar{\varepsilon}_p$ must exceed a critical fracture strain or ductility $\bar{\varepsilon}_f^*(\sigma_m/\bar{\sigma})$, **specific to the relevant stress state,** over a characteristic distance ℓ_o^* comparable with the mean spacing (d_p) of the void initiating particles, as shown schematically in Fig. 8b. Following the approach of Ritchie et al.,[29] the near-tip strain distribution $\bar{\varepsilon}_p$ from Fig. 4 is considered in terms of distance ($r = x$) directly ahead of the crack, normalized with respect to the crack tip opening displacement δ:

$$\bar{\varepsilon}_p \propto \left(\frac{J}{\sigma_o r}\right)^{\frac{1}{n+1}} \sim c_1\left(\frac{\delta}{x}\right) \quad , \tag{12}$$

where c_1 is of order unity. The crack initiation criterion of $\bar{\varepsilon}_p$ exceeding $\bar{\varepsilon}_f^*(\sigma_m/\bar{\sigma})$ over $x = \ell_o^* \sim d_p$ at $J = J_{Ic}$ now implies a ductile fracture toughness of:[29]

$$\delta_i = \delta_{Ic} \sim \bar{\varepsilon}_f^* \ell_o^* \quad , \tag{13a}$$

or $$J_{Ic} \sim \sigma_o \bar{\varepsilon}_f^* \ell_o^* \quad , \tag{13b}$$

or $$K_{Ic} \equiv \sqrt{J_{Ic} E'} \sim \sqrt{E' \sigma_o \bar{\varepsilon}_f^* \ell_o^*} \quad . \tag{13c}$$

Unlike the critical CTOD criterion (Eq. 11b), the stress-modified critical strain criterion (Eq. 13) now implies that J_{Ic} **for ductile fracture** is proportional to strength times ductility, which is more

physically realistic and permits rationalization of the toughness-strength relation for cases where microstructural changes which increase strength also cause a more rapid reduction in the critical fracture strain. Furthermore, in terms of a critical plastic zone size for Mode I fracture initiation, r_{yi}, it implies that:

$$r_{yi} \approx \frac{1}{\pi} \ell_o \frac{\bar{\varepsilon}_f^*}{\varepsilon_o} \quad , \tag{14}$$

where ε_o is the yield strain (σ_o/E), and α in Eq. (1) is taken as 0.5.

There is no conceptual difficulty with the term $\bar{\varepsilon}_f^*$, but defining it as a material constant has some difficulties in practice. It cannot, for example, necessarily be equated to either the tensile or plane strain ductilities as conventionally measured. Analysis by Rice and Tracey[37] for the rate of void expansion in the triaxial stress field ahead of a crack tip in a non-hardening material, in terms of the void radius R_p, suggests:

$$\frac{dR_p}{R_p} = 0.28\, d\bar{\varepsilon}_p \exp(1.5\, \sigma_m/\bar{\sigma}) \quad . \tag{15}$$

For an array of void initiating particles of diameter D_p and mean spacing d_p, setting the initial void radius to $D_p/2$ and integrating Eq. (15) to the point of ductile fracture initiation gives an expression for the fracture strain, $\bar{\varepsilon}_f^*$, as

$$\bar{\varepsilon}_f^* \approx \frac{\ell n(d_p/D_p)}{0.28 \exp(1.5\, \sigma_m/\bar{\sigma})} \quad . \tag{16}$$

An earlier analysis by McClintock[38] for a strain hardening material (of exponent n) containing cylindrical holes similarly suggests:

$$\bar{\varepsilon}_f^* \approx \frac{\ell n(d_p/D_p)(1 - n)}{\sinh[(1 - n)(\sigma_a^\infty + \sigma_b^\infty)/(2\bar{\sigma}/\sqrt{3})]} , \qquad (17)$$

where σ_a^∞ and σ_b^∞ are the transverse stress components.

Although both analyses consider the fracture strain to be limited by the mere impingement of the growing voids and thus tend to overestimate $\bar{\varepsilon}_f^*$ by ignoring prior coalescence due to shear banding by strain localization, they correctly suggest a dependence of $\bar{\varepsilon}_f^*$ on stress state ($\sigma_m/\bar{\sigma}$), strain hardening (n) and purity (d_p/D_p). For example, a large effect of stress state (i.e., triaxiality) on fracture strain is predicted such that from Eq. (17), $\bar{\varepsilon}_f^*$ would be expected to be reduced by an order of magnitude by going from an unnotched plane strain condition to that ahead of a sharp crack. Increased strain hardening, however, can enhance $\bar{\varepsilon}_f^*$, particularly at high triaxiality, but the benefits of increased purity (i.e., increased hole spacing d_p) are only pronounced at low D_p/d_p ratios due to the logarithmic terms in Eqs. (16) and (17). For example, reducing the volume fraction f_p of inclusions from 0.001 to 0.000001 would only increase $\bar{\varepsilon}_f^*$ by a factor of 2.[20]

More recently, a local means of evaluating $\bar{\varepsilon}_f^*$ has been suggested[41] through use of the fracture surface microroughness M, defined[42] as h/W in Fig. 9a for microvoid coalescence, and analogously[43] for other

locally-ductile fracture modes as quasi-cleavage (Fig. 7b), the tearing topography surface (TTS) and ductile intergranular, as shown in Fig. 9b. The basis for this approach is the recognition[41] that the ratio of void height h to the diameter D_p of the initiating particle is a measure of the **local** fracture strain, such that:

$$\bar{\varepsilon}_f^* \simeq \ell n(h/D_p) \quad , \tag{18}$$

or, in terms[41] of M and volume fraction f_p of void-initiating particles:

$$\bar{\varepsilon}_f^* \simeq \frac{1}{3} \ell n\left(\frac{M^2}{3f_p}\right) \quad . \tag{19}$$

Thus, Eq. (13b) would be written as:

$$J_{Ic} \sim \frac{\sigma_o}{3} \ell n\left(\frac{M^2}{3f_p}\right) \ell_o^* \quad . \tag{20}$$

The success of these microscopic models for crack initiation toughness can be appreciated in Fig. 10 where the RKR critical stress model for cleavage (Eq. 10) and stress-modified critical strain model for ductile fracture (Eq. 13) are utilized to predict the respective lower and upper shelf toughness in ASTM A533B-1 nuclear pressure vessel steel.[29] Whereas the characteristic distance (ℓ_o^*) for cleavage fracture scales approximately with 2 to 4 times the grain size (essentially the bainite packet size), for ductile fracture ℓ_o^* was

found to be approximately 5 to 6 times the average major inclusion[†] spacing (d_p).

III. CRACK GROWTH TOUGHNESS

Crack Tip Fields for Non-Stationary Cracks

Neglecting large-scale crack tip geometry changes, the plane strain near-tip stress state for the **stationary** tensile crack described above can be represented by the Prandtl slip-line field (Fig. 11a). This applies for a monotonically loaded crack under conditions of well contained yielding and at large-scale and general yielding in certain highly constrained configurations. For the **non-stationary** tensile crack, however, where applied load continuously varies with crack length, a, there are small differences in the crack tip stress field (Fig. 12). Exact asymptotic analysis by Drugan, Rice and Sham,[44] and earlier analyses by Slepyan,[45] Gao[46] and Rice and co-workers[44,47,48] for quasi-static plane strain Mode I crack advance in an elastic-perfectly plastic solid have shown that stresses are unchanged from the Prandtl field for the stationary crack (i.e., numerical solutions within $\pm$ 1 pct) except behind the tip in the neighborhood of θ = 135 deg where differences of the order of 10 pct result from the presence of a wedge of elastic unloading between approximately θ = 112 to 162 deg (Fig. 11b).

[†]The alloy contained around 0.12 vol. pct. of manganese sulphide and aluminum oxide inclusions, roughly 5 to 10 μm in diameter.

The important point, however, about this crack tip field is that the strain distribution is quite different in that, at a fixed K_I, the strain at a given distance from the crack tip in the plastic zone of a stationary crack is larger than in the case of a non-stationary crack.[44-52] This follows from the distinctly non-proportional straining of material elements above and below the crack plane for a growing crack, compared to the predominately proportional plastic straining of material elements near a stationary crack tip. As an elastic-plastic solid is more resistant to non-proportional strain histories, stable crack growth can result.[52] As shown in Fig. 4, the strains decay as 1/r ahead of a stationary crack in an elastic-perfectly plastic solid, whereas for a non-stationary crack, the strain singularity is weaker, decaying as a function of ln(1/r).

Asymptotic analyses of the strain fields for a growing Mode III crack were first reported over a decade ago by Chitaley and McClintock[49] for elastic-perfectly plastic solids, and later by Hutchinson and co-workers[51,52] for linear and power hardening solids.

For an elastic-perfectly plastic solid, the Mode III solutions for the shear strain γ_p distance r ahead of the tip are given in terms of the plastic zone size r_y and the shear yield strain $\gamma_0 = k/G$ as:[49]

$$\frac{\gamma_p}{\gamma_0} = \left(\frac{r_y}{r}\right) \quad , \qquad , \quad \text{for the stationary crack} \qquad (21)$$

$$\frac{\gamma_p}{\gamma_0} = 1 + \ell n\left(\frac{r_y'}{r}\right) + \tfrac{1}{2}\,\ell n^2\left(\frac{r_y'}{r}\right) \quad , \quad \text{for the non-stationary crack} \qquad (22)$$

where the plastic zones for stationary and growing cracks are assumed to be of equal size† and given approximately in terms of the stress intensity K_{III} as:

$$r_y = \frac{1}{\pi}\left(\frac{K_{III}}{k}\right)^2 \simeq r_y' \quad . \tag{23}$$

Although much work has been focussed on the corresponding Mode I situation,[44-48,50-52] exact asymptotic solutions for the growing plane strain tensile crack have only recently been presented by Rice, Drugan and Sham for non-hardening solids.[44] The latter solution, based on the flow theory of plasticity, shows that the opening displacement between the upper and lower crack surfaces δ very near the crack tip can be written as:[44,48]

$$\delta = \frac{\alpha r}{\sigma_o}\frac{dJ}{da} + \frac{\beta\, r\, \sigma_o}{E}\,\ell n\left(\frac{e\, r_y'}{r}\right) \quad , \quad \text{as } r \to 0 \quad , \tag{24}$$

where the proportionality factors α and β are defined numerically[44] as $\simeq 0.6$ and 5.642 (for $\nu = 0.3$), respectively, e is the natural logarithm base = 2.718 and r_y' is identified as approximately the maximum extent of the plastic zone size, given in Mode I by:

$$r_y' = \frac{s\, E\, J}{\sigma_o^2} \approx (0.11 - 0.13)\,\frac{EJ}{\sigma_o^2} \quad . \tag{25}$$

†Numerical calculations for Mode I[48] suggest that the plastic zone for the growing crack (r_y') extends roughly 15 to 30 pct beyond the stationary crack (r_y). This difference has been estimated[49] to be smaller for Mode III.

The equivalent plastic shear strain distribution at small distances r directly above and below the advancing Mode I crack tip is given, in the limit of $r \to 0$, as:[48]

$$\gamma_p = \frac{m}{\sigma_o}\frac{dJ}{da} + \frac{1.88(2 - \nu)\,\sigma_o}{E}\,\ell n\left(\frac{L}{r}\right) \quad , \tag{26}$$

where the parameters m and L are undetermined by the asymptotic analysis, although L can be identified with the extent of the plastic zone size r_y'.[53]

The form of the expressions for opening displacements δ and shear strains γ_p ahead of a growing Mode I crack (Eqs. 24 and 26, respectively) both show a first term which represents the effect of proportional plastic strain increments due to crack-tip blunting of the stationary crack whilst the second term represents the effect of additional non-proportional plastic strain increments caused by the advance of the crack, as illustrated schematically in Fig. 13.

Continuum Fracture (Macroscopic) Criteria

As noted above, the near tip vicinity of a growing tensile crack involves regions of elastic unloading and non-proportional plastic loading (Fig. 13), both of which are inadequately described by the deformation theory of plasticity upon which J is based.[10] Following the deformation theory analysis of Hutchinson and Paris,[9] which utilizes the incremental form of the HRR singularity (Eq. 3), i.e.:

$$d\varepsilon_{ij}(r,\theta) \rightarrow \left(\frac{J}{\bar{\sigma}_1 I_n r}\right)^{\frac{1}{n+1}} \left\{\frac{1}{n+1}\frac{dJ}{J} g_{ij} + \frac{da}{r} h_{ij}\right\}$$

where $$h_{ij}(\theta) = \frac{1}{n+1}\cos\theta\, g_{ij}(\theta) + \sin\theta \frac{\partial}{\partial\theta} g_{ij}(\theta) \quad , \qquad (27)$$

regions of elastic unloading, comparable with the scale of crack advance Δa, and non-proportional loading are assumed to be embedded within the HRR J-controlled singularity field of radius R (Fig. 13). Their argument for J-controlled crack extension relies on the fact that these regions remain small compared to the radius of the HRR field, such that the singularity field can be said to be controlling. For the region of elastic unloading to be small, the increment of crack extension (Δa) must be small compared with the radius of the HRR field (R), whereas for the region of non-proportionality to be small, J must increase rapidly with crack extension. With reference to the form of Eq. (27), where, similar to Eq. (26), the first term corresponds to proportional load increments and the second to non-proportional load increments, the latter condition is achieved when the proportional straining (first) term dominates, i.e., when:

$$\frac{dJ}{da} >> \frac{J}{r} \quad , \qquad (28a)$$

and $$\Delta a << R \quad , \qquad (28b)$$

Based on this non-linear elastic analysis of crack growth[9] and numerical computations by Shih and co-workers,[8], the two requirements

in Eq. (28) can be embodied into a single condition for J to uniquely characterize the near tip field of the growth crack. Thus in terms of the uncracked ligament b, J_{Ic} and the slope of the $J_R(\Delta a)$ resistance were, J-controlled growth is feasible when:

$$\omega \equiv \frac{b}{J_{Ic}} \left(\frac{dJ}{da}\right) >> 1 \quad , \tag{29}$$

where ω must exceed 10 for Prandtl field geometries (e.g., deep-cracked single-edge-notch bend) and $\sim$ 100 for center-cracked tension geometries (for $n \approx 0.1$).

A similar criterion can be applied for the asymptotic crack tip fields for elastic-ideally plastic crack growth based on flow theory (Eq. 26). For J dominated crack extension, the first term in Eq. (26), representing proportional strain increments, must dominate the second term, representing non-proportional strain increments, such that:[†]

$$\frac{dJ}{da} >> \frac{\sigma_o}{E} \ell n\left(\frac{L}{r}\right) \quad . \tag{30}$$

To provide a continuum measure of crack growth toughness, the deformation theory analysis of Hutchinson and Paris[9] is applied to define the conditions for J-controlled growth (Eq. 28) and macroscopic toughness is then assessed in terms of the tearing

[†]A similar criterion based on crack tip opening displacements implies that the crack tip opening angle $d\delta/da$ must be large compared to the yield strain σ_o/E.[8]

modulus, T_R, representing the non-dimensional slope of the $J_R(\Delta a)$ curve, $T_R = (E/\sigma_o^2)dJ/da$. Crack instability is achieved when the tearing force, $T \equiv (E/\sigma_o^2)\partial J/\partial a$ exceeds T_R. Analogous procedures[8] based on crack tip opening displacement have also been suggested in terms of the non-dimensional crack tip opening angle, defined as $d\delta/da$ normalized with respect to the yield strain σ_o/E' (Eq. 2).

However, practically speaking, the deformation theory J approach for macroscopic crack growth toughness[9] is often severely restricted by the limitation of Eq. (29). For example,[12] for a 25 mm thick 1-T compact specimen in plane strain, deformation J-controlled growth is only a reality for the first 1.5 to 2.0 mm of crack extension (i.e., where $\Delta a < 0.06b$),[8] whereas for a similar sized center-cracked tension specimen, it is valid merely for the initial 0.5 mm or so of a 25 mm ligament (i.e., where $\Delta a < 0.016b$).[8] This means that for further crack extension, the shape of the $J_R(\Delta a)$ resistance curve, and hence T_R, for a given material will differ with specimen geometry and with varying ligament size in a given geometry. To overcome this problem, Ernst[54] has recently proposed a modified J parameter, J_M, based in part on the flow theory solution for the non-stationary crack tip field (Eqs. 24-26), in which:

$$J_M = J - \int_{a_o}^{a} \left.\frac{\partial J_{pl}}{\partial a}\right|_{\delta_{pl}} da \quad , \tag{31}$$

where J_{pl} is the plastic portion of the deformation theory J, evaluated at a fixed plastic load point displacement δ_{pl} over the extent of crack

extension $(a - a_o)$. Use of this modified J-integral, J_M, and associated modified tearing moduli, has been shown to greatly extend the validity of J-controlled growth, even to situations where $\omega < 0$ and $\Delta a \approx 0.3b$ which normally would grossly violate the deformation theory requirement of Eq. (29).[54]

Local (Microscopic) Fracture Criteria

A critical strain-based microscopic criterion for ductile crack growth was first proposed by McClintock and Irwin[55] for Mode III crack extension under elastic-perfectly plastic conditions and involved the attainment of a critical shear strain γ_f^* over some characteristic radial distance $r = \ell_o^*$ into the plastic zone. Applying this local criterion for $\gamma_p > \gamma_f^*$ over distance $r = \ell_o^*$ both for crack initiation, using the Mode III plastic shear strain distribution for the stationary crack (Eq. 21), and for crack growth, using the corresponding distribution for the non-stationary crack (Eq. 22), yields estimates for the critical plastic zone sizes at initiation and instability, respectively, i.e.:

$$r_{yi} = \ell_o^* \frac{\gamma_f^*}{\gamma_o} \quad , \qquad \text{(initiation)} \qquad (32)$$

and

$$r_{yc} = \ell_o^* \exp\left[\sqrt{\frac{2\gamma_f - 1}{\gamma_o}} - 1\right] \quad , \text{(instability)} \qquad (33)$$

where γ_o is the shear yield strain. With the assumption that the critical fracture strains and distances are identical for initiation

and growth, restated in terms of K_{III} or J (using Eq. 23), this implies that stable crack growth would occur with K_{III} or J increasing from initiation values (K_i, J_i) to steady-state values (K_{ss} when such terminology is appropriate, and J_{ss}) where $dJ/da \rightarrow 0$, such that:

$$\left(\frac{K_{ss}}{K_i}\right)^2 = \frac{J_{ss}}{J_i} = \frac{\gamma_o}{\gamma_f^*} \exp\left[\sqrt{2\left(\frac{\gamma_f^*}{\gamma_o}\right) - 1} - 1\right] \quad . \qquad (34)$$

Eq. (34) implies that the potential for stable crack growth increases dramatically as γ_f^* becomes large compared to the yield strain γ_o, although subsequent analyses[52] for hardening solids has shown this potential to decrease with increases in strain hardening.

The concept of a critical strain being attained over some characteristic dimension directly **ahead** of a growing crack is not as amenable for the non-stationary Mode I case since the regions of intense strain are directly above and below the crack plane. Accordingly, Rice and his co-workers[44,47,48,50] have proposed several alternative local failure criteria for initiation and continued growth of plane strain tensile cracks, all involving the notion of a geometrically-similar crack profile very near the tip. Prior to the development of the exact asymptotic analyses for the growing Mode I crack tip fields (Eqs. 26-26), this was formulated as a constant crack tip opening angle (CTOA = $d\delta/da$) for crack growth,[9,50] as shown schematically in Fig. 14. The crack tip displacement at the advancing crack tip δ_p remains constant, whereas the crack tip displacement δ at the original crack tip is increased by the amount of opening (δ_p) to

advance the ductile crack one particle spacing $\ell_o^* \approx d_p$ for each increment of crack growth. With reference to Fig. 14, the constant crack opening angle ϕ is given by:[56,57]

$$\text{CTOA} = \phi = \arctan\left(\tfrac{1}{2} \cdot \frac{2\delta_p}{2d_p}\right) = \arctan\left(\tfrac{1}{2}\, d\delta/da\right) \quad . \quad (35)$$

Although for a rigid-plastic solid, crack advance can occur with a finite CTOA, elastic-plastic analyses result in a crack face profile with a vertical tangent immediately at the crack tip (i.e., as $r \to 0$), thus making the CTOA impossible to define numerically.[44] Accordingly Rice and Sorensen restated the crack growth criterion in more general fashion by requiring that a critical opening displacement δ_p be maintained at a small distance ℓ_o^* **behind** the crack tip.[47] With reference to Eq. (24), the local criterion of $\delta = \delta_p$ at $r = \ell_o^*$ yields:

$$\frac{\delta_p}{\ell_o^*} = \frac{\alpha}{\sigma_o}\frac{dJ}{da} + \beta\,\frac{\sigma_o}{E}\,\ell n\left(\frac{e\, r_y'}{\ell_o^*}\right) \quad . \quad (36)$$

By comparing Figs. 9 and 14, it is apparent that the left side of Eq. (36), the ratio of local microscopic parameters, δ_p/ℓ_o^*, can be identified with the fracture surface microroughness, M = h/w, for microvoid coalescence and possibly other modes. This point is further discussed in the following section. Rice and co-workers,[48] however, have rephrased this geometrically-similar near tip profile criterion to

remove reference to the local microscopic parameters δ_p and ℓ_o^*, by noting that Eq. (24) can be rewritten as:

$$\delta = \beta\, r\, \frac{\sigma_o}{E}\, \ell n\, \frac{\rho}{r} \quad , \qquad r \to 0 \tag{37}$$

with $$\rho \equiv r_y' \exp\{\frac{\alpha}{\beta}(\frac{E}{\sigma_o^2})\, \frac{dJ}{da}\} \tag{38a}$$

$$\equiv r_y' \exp(1 + \frac{\alpha}{\beta}\, T_R) \quad , \tag{38b}$$

where T_R is the tearing modulus. Since the parameter ρ fully characterizes the near tip crack tip profile, Rice et al.[48] proposed ρ = constant as a criterion for continued growth. Evaluating under ssy conditions at the onset of growth $a = a_o$ at $J = J_{Ic}$ yields:

$$\rho = \frac{s\, E\, J_{Ic}}{\sigma_o^2}\, (1 + \frac{\alpha_{ssy}}{\beta}\, T_o) \quad , \tag{39}$$

where α_{ssy} (≈ 0.58) is the value of α appropriate to ssy and T_o is the initial value of the tearing modulus given by:

$$T_o = \frac{E}{\alpha_{ssy}\, \sigma_o} \cdot \frac{\delta_p}{\ell_o^*} - \frac{\beta}{\alpha_{ssy}}\, \ell n(\frac{e\, s\, E\, J_{Ic}}{\ell_o^*\, \sigma_o^2}) \quad . \tag{40}$$

This implies a general growth criterion valid for ssy and fully plastic conditions of:[48]

$$T_R \equiv \frac{E}{\sigma_o^2}\, \frac{dJ}{da} = \frac{\alpha_{ssy}}{\alpha}\, T_o - \frac{\beta}{\alpha}\, \ell n(\frac{r_y'}{s\, E\, J_{Ic}/\sigma_o^2}) \quad , \tag{41}$$

which provides the differential equation governing plane strain tensile crack growth with increase in J from initiation at $J_i = J_{Ic}$ to the steady state value J_{ss} where a plateau in the $J_R(\Delta a)$ curve will be reached (i.e., as $dJ/da \rightarrow 0$). For small-scale yielding with $\nu = 0.3$, this gives:

$$\frac{J_{ss}}{J_{Ic}} = \exp\left(\frac{\alpha_{ssy}}{\beta} T_o\right) = \exp(0.1\ T_o) \quad . \tag{42}$$

Although the "constant ρ" criterion for continued Mode I crack extension has been found to be consistent with experimental $J_R(\Delta a)$ measurements, i.e., in deeply-cracked bend tests on AISI 4140 steel (σ_o = 1250 MPa),[58] the approach is essentially not microscopically based. A more physically realistic approach[53] is to consider a local fracture criterion, similar to the Mode III case (Eqs. 32 and 33), where crack advance is consistent with the attainment of a critical accumulated plastic strain, γ_f^*, within a microstructurally characteristic radial distance ℓ_o^* from the crack tip.[20,38,55] By analogy to Mode III,[20,38,53] the local criterion of $\gamma_p > \gamma_f^*$ over radial distance $r = \ell_o^*$ is applied for both Mode I initiation, using the strain distribution for a stationary crack (Eq. 12 and Fig. 4), and continued growth and instability using the non-stationary crack strain distribution in Eq. (24). This yields estimates for the critical plastic zone sizes for Mode I crack initiation (r_{yi}) and instability (r_{yc}) as:

$$r_{yi} \approx \ell_o^* \left[\frac{1}{\pi} \frac{\bar{\varepsilon}_f^*}{\varepsilon_o}\right] \quad , \qquad \text{(initiation)} \quad (43)$$

$$r_{yc} \approx \ell_o^* \exp\left[\frac{0.6(1 + \nu)}{(2 - \nu)} \frac{\bar{\varepsilon}_f^*}{\varepsilon_o}\right] \quad , \qquad \text{(instability)} \quad (44)$$

where the instability result is derived from Eq. (24) assuming sufficient plasticity during crack advance such that the second term in the shear strain distribution, representing non-proportional strain increments, dominates the first term, representing proportional strain increments (i.e., the inverse of Eq. 28). It should be noted that, similar to the Mode III expressions (Eqs. 32 and 33), the critical plastic zone size for the growing crack is an exponential function of the ratio of fracture to yield strain, rather than a direct function for crack initiation. However, unlike Mode III, there is no square root dependence in the exponential term (see also ref. 53). Although the numerical constants are only approximate,† this implies that for Mode I cracks:

$$\left(\frac{K_{ss}}{K_i}\right)^2 = \frac{J_{ss}}{J_i} \approx \pi \frac{\varepsilon_o}{\bar{\varepsilon}_f^*} \exp\left[0.6 \frac{\bar{\varepsilon}_f^*}{\varepsilon_o}\right] \quad , \qquad (45)$$

Similar to the Mode III case, a comparison of the microscopically-based relationships for crack initiation and instability in Mode I

†Since for Mode I cracks, plastic zones extend principally at an angle to the crack plane, rather than directly ahead, the critical strain criteria should be applied at such angles.[53] In reality this results in the zig-zag crack path morphology of ductile fracture in Mode I, which is frequently observed in higher strength (lower n) materials.[59]

(i.e., Eqs. 43-45) clearly shows that microstructural changes in a material which increase the fracture ductility and decrease the yield strength (i.e., lower ε_o) can have a much larger (beneficial) effect on crack growth toughness as opposed to crack initiation toughness. This can be appreciated by comparing experimental J_{Ic} and $J_R(\Delta a)$ data.[59-63] For example, Fig. 2 shows Wilson's $J_R(\Delta a)$ resistance curves for A516 Grade 70 steels following various steelmaking processes to control the inclusion content.[63] It is apparent that the effect of controlling the volume fraction and shape of oxides and sulphides through additional calcium treatments (CaT), compared to conventional vacuum degassing (CON) only, becomes progressively more significant with increasing crack extension. According to the simple modelling analysis described above, this can result simply from the different strain distributions for the stationary and running crack (i.e., c.f., Eqs. 12 and 26, or Eqs. 21 and 22) rather than from any change in the local fracture criteria.

IV. RELATIONSHIP BETWEEN T_R AND J_{Ic}

Conventionally, correlations between various toughness parameters have been made in purely empirical fashion through regression analysis to experimental data. For example, the many (often dimensionally incorrect) expressions purporting to define relationships between K_{Ic} and Charpy V-notch impact energy have been obtained exactly in this manner.[64] However, the failure criteria reviewed above for both initiating and growing cracks provide an ideal physical basis for

examining the relationship between crack initiation and growth toughness parameters without recourse to such purely empirical procedures. Specifically the model of Rice et al.[44,48] of the geometrically-similar very near crack tip profile of an extending crack within the asymptotic Mode I deformation field of the non-stationary flaw permits a logical correlation of J_{Ic} and the tearing modulus T_R, as previously noted by Shih et al.[13] Following Rice et al.,[48] the general expression for T_R (Eq. 41), when evaluated under small-scale yielding conditions, simplifies to:

$$T_R \equiv \frac{E}{\sigma_o^2} \cdot \frac{dJ}{da} = T_o - \frac{\beta}{\alpha_{ssy}} \ell n\left(\frac{J}{J_{Ic}}\right) \quad . \qquad (46)$$

Under fully plastic conditions, where the "plastic zone" dimension r_y' is considered to saturate with full yielding at some fraction of the uncracked ligament ($r_y' \sim b/4$), Eq. (41) becomes:[48]

$$T_R \equiv \frac{E}{\sigma_o^2} \cdot \frac{dJ}{da} = \frac{\alpha_{ssy}}{\alpha_{fp}} \left[T_o - \frac{\beta}{\alpha_{ssy}} \ell n\left(\frac{b/4}{s\, E\, J_{Ic}/\sigma_o^2}\right)\right] \quad , \quad (47)$$

where for fully yielded conditions $\alpha_{fp} \approx 0.51$.

Since the parameters α_{ssy}, α_{fp}, β and s have all been determined to a fair degree of accuracy by finite element computations,[44] the major problem in utilizing Eqs. (46) and (47) to relate J_{Ic} and T_R reduces to interpreting quantitatively the microscale parameters δ_p and ℓ_o^*. Dean and Hutchinson[52] suggest that the ratio δ_o/ℓ_o^*, normalized with respect to the yield strain, should exceed 100 for intermediate strength

steels. When δ_p/ℓ_o^* can be equated to the microroughness parameter M (Figs. 9 and 14), this implies M values greater than 0.16 (for 350 MPa yield strength) to 0.50 (for 1000 MPa yield strength). These values are consistent with available experimental data.[41,42] Sorensen and Rice.[47] on the other hand, equate ℓ_o^* with the fracture process zone size, which for microvoid coalescence is taken of the order of the spacing d_p of the void initiating particles (e.g., Fig. 14). Since from Rice and Johnson's analysis,[22] the CTOD at initiation, δ_i, should be in the range of 0.5 to 2.0 d_p (Eq. 11), it was suggested[47] that δ_p be regarded as an independent empirical parameter and that ℓ_o^* be taken to be of the order of 0.5 to 2.0 δ_i. Ordinarily, one would regard both d_p and ℓ_o^* as material parameters, so this implicit assumption of $\delta_p/\ell_o^* = 1$ seems artificially restrictive. In fact, in terms of the fracture surface microroughness, it implies M values of order unity, which appears[41-43] to be an upper limit for fully plastic conditions unless particles are rare.

To simplify the functional form of the expressions between J_{Ic} and T_R, we alternatively utilize the crack growth data of Green and Knott and others[56,57,60,65,66] and note that the additional CTOD at the advancing crack tip δ_p is smaller than the CTOD δ_i to cause initiation at the original crack tip, i.e., with reference to Fig. 14:

$$\delta_p = \lambda \delta_i = \frac{\lambda \alpha J_{Ic}}{\sigma_o} , \qquad (48)$$

where λ is of the order of, yet less than, unity. Note that, to the

extent that $\delta_i \propto d_p$, λ can be taken as proportional to 1/M. Incorporating Eq. (48) into Eqs. (46) and (47) yields, for small-scale yielding:

$$T_R = \lambda\left(\frac{J_{Ic}\,E}{\ell_o^*\,\sigma_o^2}\right) - \frac{\beta}{\alpha_{ssy}}\,\ell n\left[es\left(\frac{J_{Ic}\,E}{\ell_o^*\,\sigma_o^2}\right)\right] - \frac{\beta}{\alpha_{ssy}}\,\ell n\left(\frac{J}{J_{Ic}}\right) \quad , \quad (49)$$

and for large-scale yielding:

$$T_R = \frac{\alpha_{ssy}}{\alpha_{fp}}\left[\lambda\left(\frac{J_{Ic}\,E}{\ell_o^*\,\sigma_o^2}\right)\right] - \frac{\beta}{\alpha_{ssy}}\,\ell n\left[es\left(\frac{J_{Ic}\,E}{\ell_o^*\,\sigma_o^2}\right)\right] + \frac{\beta}{\alpha}\,\ell n\left[\frac{4s\,\ell_o^*}{b}\left(\frac{J_{Ic}\,E}{\ell_o^*\,\sigma_o^2}\right)\right] \quad . \quad (50)$$

Using the most recently reported values for the parameters α_{ssy}, α_{fp}, β, e and s from finite element computations,[44] and taking realistically $\lambda \sim 0.2$, the variations in T_R values with non-dimensional J_{Ic} values predicted from Eqs. (49) and (50) are shown in Fig. 15 for conditions of small-scale yielding and full plasticity.† For the former ssy condition, curves are shown at the onset of growth, i.e., at $J/J_{Ic} = 1$ when $T = T_o$, and when J values are an order of magnitude larger than the initiation value. For full yielding, the T_R vs. J_{Ic} expression is evaluated for both 30 mm and 120 mm uncracked ligaments,

†A previous approach by Shih et al.,[13] utilizing the earlier formulation of Rice and Sorensen[47] for the crack tip fields in ssy, used an assigned value of ℓ_o^* of 700 μm. For the materials considered, however, this value of ℓ_o^* was clearly much larger than d_p.

which represent typical values of b in one inch (25 mm) and four inch (102 mm) thick compact specimens pre-cracked to an a/W of $\sim$ 0.6. However, it is clear that in each case these logarithmic third terms in Eqs. (49) and (50) have only a marginal influence for the range of values quoted.

Using the experimental toughness data in refs. 7, 63, 67, and 68 for a wide variety of steels ranging from low to high strength (i.e., σ_o/E values from 0.002 to 0.006[†]), Eqs. (49) and (50) can be seen in Fig. 15 to provide an excellent basis for comparison of J_{Ic} and T_R, except perhaps at very high tearing modulus values exceeding 300 or so. It should be noted, however, that in the construction of Fig. 15, the characteristic dimension ℓ_o^*, which was used as a fitting parameter, was assigned a value of 130 μm. Although the basis for this is arbitrary, in keeping with the physical idealization of ductile crack growth depicted in Fig. 14, it is apparent that this size should be comparable with the mean inclusion spacing in these pressure vessel steels, such that ℓ_o^* will be of the order of d_p. The spacing of <u>all</u> inclusions in such steels is far below 130 μm, but d_p may correspond to the largest, earliest-initiating inclusions.[42] If these have a volume fraction of 2 pct, for example, their size for a 130 μm spacing would have to be about 25 μm, a large but not unreasonable number.

[†]As in customary practice, the flow stress σ_o is taken as the mean of the tensile yield and ultimate tensile stresses.

Thus, as noted previously,[13] both experimental data and analytical predictions show a trend of virtually a linear increase in crack growth toughness $T_R \equiv (E/\sigma_o^2)(dJ/da)$, with increase in the non-dimensional crack initiation toughness, J_{Ic}. Experimental results[56,57,60-62,69,70] with crack tip opening displacement measurements similarly show a general increase in $d\delta/da$ with increase in δ_i.

Another approach to evaluating Eqs. (49) and (50) could be developed through measurements of M, which can most confidently be done for microvoid coalescence fractures. Measurement of d_p, δ_i and M together would also provide a means of assessing whether $\lambda \propto 1/M$ in general and whether the constant of proportionality is a material parameter. As pointed out elsewhere in more detail,[41,42] M reflects local fracture conditions in the crack tip process zone, and therefore offers a more direct means of assessing d_p and δ_p than macroscopic measurements. In this connection, it is important to recognize that d_p must refer, not to a metallographic spacing of all particles in the material, but to the spacing of those particles which are "effective" in the fracture process.[42] The effective particles may not include all which de-bond from the matrix in crack extension, but only those which nucleate early enough in the strain to fracture to drive the necking, shear localization, or both, of the interparticle ligaments. M is a much more promising approach to determination of such parameters than is conventional metallography; the estimate above, of a 25 μm diameter for "critical" inclusions, was made in this spirit.

When fracture does not proceed by microvoid coalescence, the analysis is necessarily complicated by less complete understanding of microstructural nuclei.[43,71] However, one important case in structural alloys is that of "blocky" fracture surfaces, which comprise not only the microroughness depicted in Fig. 9, but also a "regional" roughness on a scale of tends to hundreds of dimple or ridge spacings. This roughness scale can be described analogously to Fig. 9, as has been pointed out.[43] Moreover, there may be a large-scale component to ℓ_o^* for such fractures.

The foregoing implicitly assumes that material characteristics determine d_p and δ_p (for a given crack tip stress state), while ℓ_o^* would correspond to a particular fracture micromechanism in that material. It is tempting to guess that ℓ_o^* would typically be a small, integer multiple of a well-defined microstructural dimension, as in the RKR result,[27] but in fact the general case may be a wide range in relative size scales, depending on whether the fracture is locally controlled, as seems to be the case in microvoid coalescence and TTS fractures,[43,72] or is partly regionally controlled, as in blocky fractures, ductile intergranular fractures, and in quasi-cleavage.[43,73] At the present level of understanding, it appears more appropriate to attempt to measure d_p and regard ℓ_o^* as a fitting parameter which both depends on the particular fracture micromechanism and also must exhibit a size scale consistent with that micromechanism and the relevant microstructural features.

V. CONCLUDING REMARKS

In this paper, the distinction between fracture toughness associated with crack initiation and associated with subsequent slow crack growth has been examined on the basis of differences between the stress and deformation fields local to the crack tip regions of stationary and non-stationary Mode I cracks. Both macroscopic descriptions, based on continuum fracture mechanics where field parameters are used to globally characterize such fields for crack initiation (i.e., $K_I = K_{Ic}$ or $J = J_{Ic}$) and for crack growth (i.e., at instability $T = T_R$), and microscopic descriptions, based on local failure criteria for specific fracture mechanisms (transgranular cleavage and principally microvoid coalescence), have been compared. By considering a critical strain micromechanical model for void coalescence,[38,39] it was found that metallurgical factors which specifically influence yield strength (σ_o) and local fracture ductility ($\bar{\varepsilon}_f^*$) can have a far greater influence on crack growth toughness (e.g, T_R) compared to crack initiation toughness (e.g., J_{Ic}); a result which is principally a consequence of the weaker strain singularity ahead of a slowly growing tensile crack and is analogous to the previous result by McClintock and co-workers in Mode III.[20,49,55] Furthermore, by considering a similar micromechanical model for crack growth based on the attainment of a geometrically similar crack tip profile,[48] a relationship between the tearing modulus T_R and the crack initiation fracture toughness J_{Ic} was described and found to provide a good fit to

experimental toughness data on a wide range of steels. Finally, it was briefly shown that many of the microscopic parameters describing local conditions of fracture in the crack tip vicinity, such as the local fracture strains ($\bar{\varepsilon}_f^*$), local crack tip displacements (δ_p) and microstructurally-significant dimensions (ℓ_o^*), which are not readily ammenable to experimental measurement, can be deduced from quantitative analysis of fracture surface morphology, specifically involving the microroughness.[42]

Such analyses highlight the significance of the non-stationary crack tip fields to the modelling and continuum description of sub-critical crack growth where the presence of crack tip plasticity and associated plastic zones in the wake of the crack tip lead to lower strains at the same nominal driving force, i.e., same K_I or J, than that predicted by the currently-used stationary crack analyses. For strain-controlled fracture, this effect results in resistance curve behavior where an increasing nominal driving force, i.e., increasing K_I or J, must be applied to sustain crack extension, even though the failure criterion can remain unchanged. Furthermore, the enhanced role of microstructure in influencing resistance to crack growth, compared to crack initiation, which follows from this modified strain distribution for slowly moving cracks, implies that fracture toughness, when assessed in terms of crack growth parameters such as the tearing modulus T_R, becomes far more amenable to metallurgical control.

NOMENCLATURE

a	crack length
a	initial crack length
B, b	test piece thickness and uncracked ligament, respectively
c_i	constant in Eq. (12)
CTOA	crack tip opening angle ($d\delta/da$)
CTOD	crack tip opening displacement (δ)
d_g	grain size
d_p, D_p	particle spacing and diameter, respectively
E	elastic (Young's) modulus
E'	$= E/1 - \nu^2$ in plane strain, and E in plane stress
e	natural logarithm base (= 2.718)
f_p	volume fraction of particles
f_{ij}, g_{ij}, h_{ij}	universal functions of θ in Eqs. (3) and (27)
G	elastic shear modulus
h	height of fracture surface asperity (Fig. 9)
I_n	numerical constant in HRR solution, weakly dependent upon n
J	J-integral
J_i	critical J value at crack initiation
J_{Ic}	plane strain fracture toughness, defined at crack initiation in Mode I

J_M, J_{pl}	modified and plastic portion of deformation theory J, respectively
$J_R(\Delta a)$	J-resistance curve
J_{ss}	steady-state J when $dJ/da \rightarrow 0$
k	shear yield stress
K_I, K_{III}	linear elastic stress intensity factor in Modes I and III, respectively
K_i	critical value of K_I at crack initiation
K_{Ic}	plane strain fracture toughness, defined for ssy at crack initiation in Mode I
K_{ss}	steady-state K_I at $dK/da \rightarrow 0$
ℓ_o^*	characteristic dimension for fracture
L	parameter in non-stationary crack tip strain field related to r_y' (Eq. 26)
m	parameter in Eq. (26)
M	fracture surface microroughness (= h/w)
n	strain hardening exponent in $\bar{\sigma} = \sigma_1 (\bar{\varepsilon}_p)^n$
r	radial distance ahead of crack tip
r_y, r_y'	plastic zone size for stationary and non-stationary cracks, respectively
r_{yi}, r_{yc}	critical plastic zone size at crack initiation and instability, respectively
R	radius of HRR crack tip field
R_p	radius of void
s	constant (= 0.11 to 0.13) relating J and r_y'

T	tearing force (= $(E/\sigma_o^2)\partial J/\partial a$)
T_R	tearing modulus (= $(E/\sigma_o^2)dJ/da$)
T_o	initial value of tearing modulus at $J = J_{Ic}$
u_i	displacement ahead of crack tip
w	width of fracture surface asperity (Fig. 9)
x	distance directly ahead of crack tip at $\theta = 0$
α_{ssy}, α_{fp}	small-scale yielding and fully plastic values of α, respectively
α	constant relating δ to J
β	constant in Eq. (24) (= 5.642 for $\nu = 0.3$)
γ_p	plastic shear strain
γ_f^*, γ_o	critical local fracture strain and yield strain, respectively
δ	crack tip opening displacement (CTOD)
δ_{Ic}	CTOD at crack initiation in plane strain
δ_i, δ_p	CTOD's for crack initiation and propagation, respectively
δ_{pl}	plastic load point displacement
$\delta_R(\Delta a)$	CTOD resistance curve
$\bar{\varepsilon}_p$	equivalent plastic strain
ε_{ij}^p	plastic strains ahead of crack tip
ε_f^*, ε_o	critical local fracture strain and yield strain, respectively
$\tilde{\varepsilon}_{ij}, \tilde{\sigma}_{ij}, \tilde{u}_i$	normalized strain, stress and displacement functions of θ in Eq. (5)

ϕ	half crack tip opening angle
λ	constant relating δ_i and δ_p
ν	Poisson's ratio
ρ	parameter characterizing near tip profile of non-stationary crack
$\bar{\sigma}$	equivalent (or effective) stress
σ_a^∞, σ_b^∞	transverse stress components
σ_f^*, σ_o	critical local fracture stress and flow stress, respectively
σ_m	hydrostatic stress (mean normal stress = $\sum_{i=1}^{3} \sigma_{ij}$)
σ_{ij}	stresses ahead of crack tip
σ_{yy}	local tensile opening stress ahead of crack tip
$\bar{\sigma}_1$	equivalent stress at unit strain
θ	angle measured from crack tip from plane of crack.

ACKNOWLEDGEMENTS

This work was supported by the Director, Office of Energy Research, Office of Basic Energy Sciences, Materials Science Division of the U.S. Department of Energy under Contract No. DE-AC03-76SF00098 (R.O.R.) and by the U.S. National Science Foundation under Grant No. 81-19541 (A.W.T.). Thanks are particularly due to Dr. George Green and Professor F. A. McClintock for many informative discussions, and to Dr. J. F. Knott for providing the micrograph in Fig. 14d.

REFERENCES

1. ASTM E399-83, in Standard Test Method for Plane Strain Fracture Toughness of Metallic Materials, 1983 Annual Book of ASTM Standards, Section 3, American Society for Testing and Materials, Philadelphia, PA, 1983, pp. 170-553.

2. ASTM E813-81, in Standard Test Method for J_{Ic}, a Measure of Fracture Toughness, ibid, pp. 762-780.

3. J. A. Begley and J. D. Landes: in Fracture Toughness, ASTM STP 514, American Society for Testing and Materials, Philadelphia, PA, 1974, pp. 170-186.

4. J. F. Knott: in Fundamentals of Fracture Mechanics, Butterworths, London, 1973.

5. C. F. Shih: J. Mech. Phys. Solids, 1981, vol. 29, pp. 305-330.

6. J. R. Rice: in The Mechanics of Fracture, F. Erdogan, ed., American Society for Mechanical Engineers, Warrendale, PA, 1976.

7. P. C. Paris, H. Tada, A. Zahoor and H. Ernst: in Elastic-Plastic Fracture, ASTM STP 668, American Society for Testing and Materials, Philadelphia, PA, 1979, pp. 5-36.

8. C. F. Shih, H. G. de Lorenzi and W. R. Andrews: ibid., pp. 65-120.

9. F. A. McClintock: in Physics of Strength and Plasticity, A. S. Argon, ed., M.I.T. Press, Cambridge, MA, 1969, pp. 307-326.

10. J. W. Hutchinson and P. C. Paris: in Elastic-Plastic Fracture, ASTM STP 668, American Society for Testing and Materials, Philadelphia, PA, 1979, pp. 37-64.

11. J. W. Hutchinson: in Non Linear Fracture Mechanics, Department of Solid Mechanics, The Tech. Univ. of Denmark, 1979.

12. R. O. Ritchie: J. Eng. Matls. Tech., Trans. ASME Series H, 1983, vol. 105, pp. 1-7.

13. C. F. Shih, W. R. Andrews and J. P. D. Wilkenson: in Mechanical Behavior of Materials, Proc. 3rd Intl. Conf., K. J. Miller and R. F. Smith, eds., Pergamon Press, Oxford, 1980, vol. 3, pp. 589-601.

14. M. L. Williams: J. Applied Mech., Trans. ASME, 1957, vol. 24, pp. 109-114.

15. G. R. Irwin: in Fracture, Handbook of Physics, Pringer, Berlin, 1958, vol. 6.

16. J. W. Hutchinson: J. Mech. Phys. Solids, 1968, vol. 16, pp. 13-31.

17. J. R. Rice and G. R. Rosengren: ibid., pp. 1-12.

18. J. R. Rice: J. Applied Mech., Trans. ASME Series E, 1968, vol. 35, pp. 379-386.

19. C. F. Shih: in Fracture Analysis, ASTM STP 560, American Society for Testing and Materials, Philadelphia, PA, 1974, pp. 187-210.

20. F. A. McClintock: in Fundamental Aspects of Structural Alloy Design, R. I. Jaffee and B. A. Wilcox, eds., Plenum, New York, 1977, pp. 147-172.

21. C. F. Shih: Division of Engineering, Brown University Report No. MRL E-147, June 1983, Providence, RI.

22. J. R. Rice and M. A. Johnson: in Inelastic Behavior of Solids, M. F. Kanninen, W. G. Adler, A. R. Rosenfield and R. I. Jaffee, eds., McGraw-Hill, New York, 1970, pp. 641-672.

23. R. M. McMeeking: J. Mech. Phys. Solids, 1977, vol. 25, pp. 357-381.

24. D. M. Tracey: J. Eng. Matls. Tech., Trans. ASME Series H, 1976, vol. 98, pp. 146-151.

25. F. A. McClintock: in Fracture, An Advanced Treatise, H. Liebowitz, ed., Academic Press, New York, 1968, vol. 3, pp. 47-158.

26. R. M. McMeeking and D. M. Parks: in Elastic-Plastic Fracture, ASTM STP 668, American Society for Testing and Materials, Philadelphia, PA, 1979, pp. 175-194.

27. R. O. Ritchie, J. F. Knott and J. R. Rice: J. Mech. Phys. Solids, 1973, vol. 21, pp. 395-410.

28. D. A. Curry: Met. Sci., 1980, vol. 14, p. 319.

29. R. O. Ritchie, W. L. Server and R. A. Wullaert: Metall. Trans. A, 1979, vol. 10A, pp. 1557-1570.

30. A. G. Evans: Metall. Trans. A, 1983, vol. 14A, pp. 1349-1355.

31. D. A. Curry: Mater. Sci. Eng., 1980, vol. 43, pp. 135-144.

32. D. M. Parks: J. Eng. Matls. Tech., Trans. ASME Series H, 1976, vol. 98, pp. 30-35.

33. D. A. Curry: CERL Report No. RD/L/N103/79, Central Electricity Generating Board, Sept. 1979, Leatherhead, UK.

34. R. O. Ritchie, L. C. E. Geniets and J. F. Knott: in The Microstructure and Design of Alloys, Proc. 3rd Intl. Conf. Strength Metals and Alloys, 1973, vol. 1, pp. 124-128, Institute of Metals/Iron and Steel Institute, London.

35. J. Kameda and C. J. McMahon: Metall. Trans. A, 1980, vol. 11A, pp. 91-101.

36. K. N. Akhurst and T. J. Baker: Metall. Trans. A, 1981, vol. 12A, pp. 1059-1070.

37. J. R. Rice and D. M. Tracey: J. Mech. Phys. Solids, 1969, vol. 17, pp. 201-217.

38. F. A. McClintock: J. Applied Mech., Trans. ASME Series H, 1958, vol. 25, pp. 363-371.

39. A. C. Mackenzie, J. W. Hancock and D. K. Brown: Eng. Fract. Mech., 1977, vol. 9, pp. 167-188.

40. R. C. Bates: in Metallurgical Treatises, J. K. Tien and J. F. Elliott, eds., TMS-AIME, Warrendale, PA, 1982, pp. 551-570.

41. A. W. Thompson and M. F. Ashby: Scripta Met., 1983, in review.

42. A. W. Thompson: Acta Met., 1983, vol. 31, pp. 1517-1523.

43. A. W. Thompson: Proc. 6th Intl. Conf. on Fracture, India, S. R. Valluri, ed., Pergamon Press, Oxford, 1984, in review.

44. W. J. Drugan, J. R. Rice and T.-L. Sham: J. Mech. Phys. Solids, 1982, vol. 30, pp. 447-473.

45. L. I. Slepyan: Izv. Akad. Nauk. SSSR Mekhanika Tverdogo Tela, 1974, vol. 9, pp. 57-67 (quoted in ref. 44).

46. Y.-C. Gao: in Elastic-Plastic Fracture, ASTM STP 803, C. F. Shih and J. P. Gudas, eds., American Society for Testing and Materials, Philadelphia, PA, 1983.

47. J. R. Rice and E. P. Sorensen: J. Mech. Phys. Solids, 1978, vol. 26, pp. 163-186.

48. J. R. Rice, W. J. Drugan and T.-L. Sham: in Fracture Mechanics, 12th Conf., ASTM STP 700, American Society for Testing and Materials, Philadelphia, PA, 1980, pp. 189-221.

49. A. D. Chitaley and F. A. McClintock: J. Mech. Phys. Solids, 1971, vol. 19, pp. 147-163.

50. J. R. Rice: in Mechanics and Mechanisms of Crack Growth, M. J. May, ed., 1974, pp. 14-39, British Steel Corp., London.

51. J. C. Amazigo and J. W. Hutchinson: J. Mech. Phys. Solids, 1977, vol. 25, pp. 81-97.

52. R. H. Dean and J. W. Hutchinson: in Fracture Mechanics, 12th Conf., ASTM STP 700, American Society for Testing and Materials, Philadelphia, PA, 1980, pp. 383-405.

53. F. A. McClintock: "Predicting Elastic-Plastic and Fully Plastic Fracture from Hole Growth Mechanisms," M.I.T. Technical Report, June 1981, Dept. of Mechanical Engineering, M.I.T., Cambridge, Mass.

54. H. A. Ernst: in Elastic-Plastic Fracture: Second Symposium. Volume I - Inelastic Crack Analysis, ASTM STP 803, C. F. Shih and J. P. Gudas, eds., American Society for Testing and Materials, Philadelphia, PA, 1983, pp. I191-I213.

55. F. A. McClintock and G. R. Irwin: in Fracture Toughness Testing and its Applications, ASTM STP 381, American Society for Testing and Materials, Philadelphia, PA, 1965, pp. 84-113.

56. G. Green and J. F. Knott: J. Mech. Phys. Solids, 1975, vol. 23, pp. 167-183.

57. G. Green and J. F. Knott: J. Eng. Matls. Tech., Trans. ASME Series H, 1976, vol. 98, pp. 37-46.

58. L. Hermann and J. R. Rice: Met. Sci., 1980, vol. 14, pp. 285-291.

59. J. Q. Clayton and J. F. Knott: Met. Sci., 1976, vol. 10, p. 63.

60. A. A. Willoughby, S. J. Garwood and C. E. Turner: in Advances in Fracture Research, Proc. 5th Intl. Conf. on Fracture, D. Francois, ed., Pergamon Press, Oxford, 1981, vol. 1, pp. 179-186.

61. G. Green and A. A. Willoughby: CEGB South Western Region Report No. SSD/SW/79/R339, March 1980, Central Electricity Generating Board, London HQ, U.K.

62. G. Green: CEGB South Western Report No. SSD/SW/80/R343, May 1980, Central Electricity Generating Board, London HQ, U.K.

63. A. D. Wilson: J. Eng. Matls. Tech., Trans. ASME Series H, 1979, vol. 101, pp. 265-274.

64. S. T. Rolfe and J. M. Barsom: in Fracture and Fatigue Control in Structures, Prentice-Hall, Englewood Cliffs, NJ, 1977.

65. G. Berry and R. Brook: Int. J. Fracture, 1975, vol. 11, p. 993.

66. S. J. Garwood and C. E. Turner: ibid., 1978, vol. 14, p. R195.

67. M. G. Vassilaros, J. A. Joyce and J. P. Gudas: in Fracture Mechanics, 14th Symp.: Vol. 1. Theory and Analysis, ASTM STP 791, J. C. Lewis and G. Sines, eds., American Society for Testing and Materials, Philadelphia, PA, 1983, pp. I65-I83.

68. J. A. Joyce: ibid., pp. I543-I560.

69. G. Clark, S. M. El Soudani, W. G. Ferguson, R. F. Smith and J. F. Knott: in Ductile Crack Extension in Pressure Vessel Steels, Institution of Mechanical Engineering, London, 1978.

70. G. A. Clarke, W. R. Andrews, P. C. Paris and D. W. Schmidt: in Mechanics of Crack Growth, ASTM STP 590, American Society for Testing and Materials, Philadelphia, PA, 1976, pp. 27-42.

71. A. W. Thompson and I. M. Bernstein: in Hydrogen Effects in Metals, TMS-AIME, Warrendale, PA, 1981, pp. 291-308.

72. A. W. Thompson and J. C. Chesnutt: Metall. Trans. A, 1979, vol. 10A, pp. 1193-1196.

73. C. D. Beachem and R. M. N. Pelloux: in Fracture Toughness Testing and Its Applications, ASTM STP 381, American Society for Testing and Materials, Philadelphia, PA, 1965, pp. 210-244.

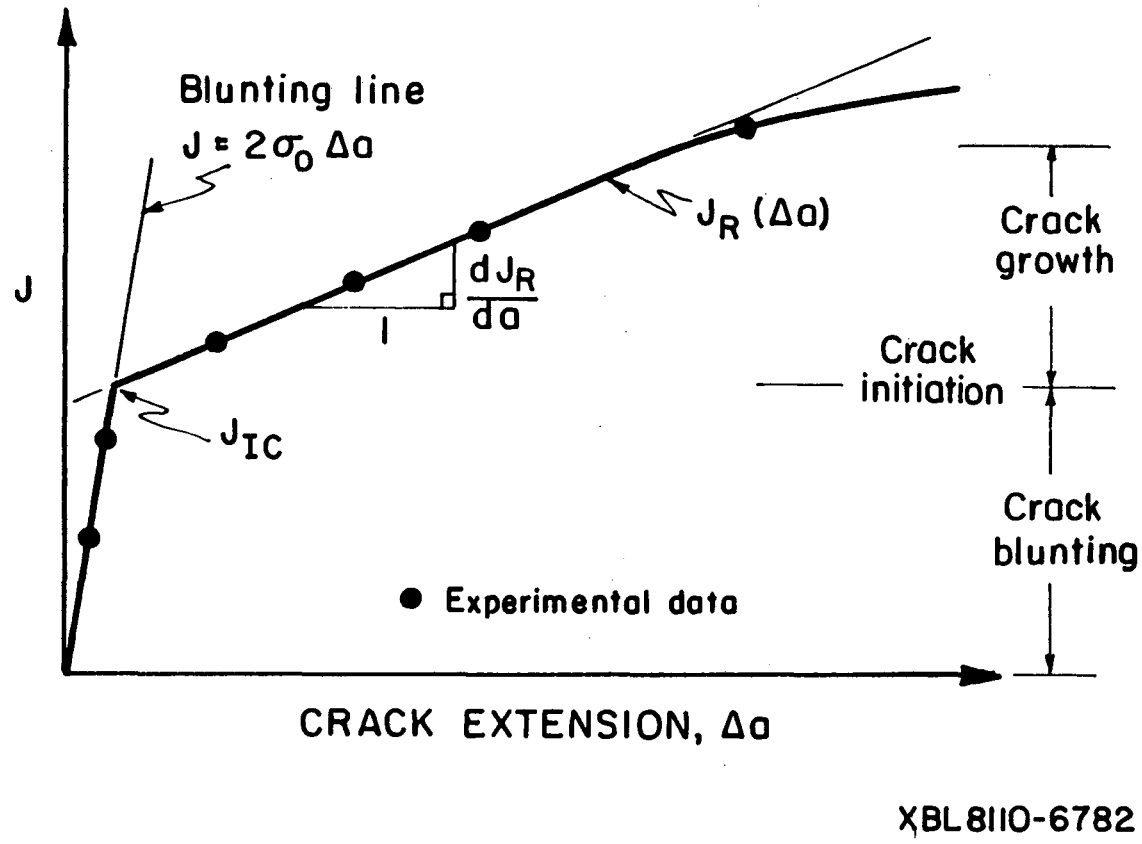

Fig. 1: $J_R(\Delta a)$ resistance curve of J versus crack extension Δa, showing definition of $J_j = J_{IC}$ at initiation of crack growth where the blunting line intersects the resistance curve.

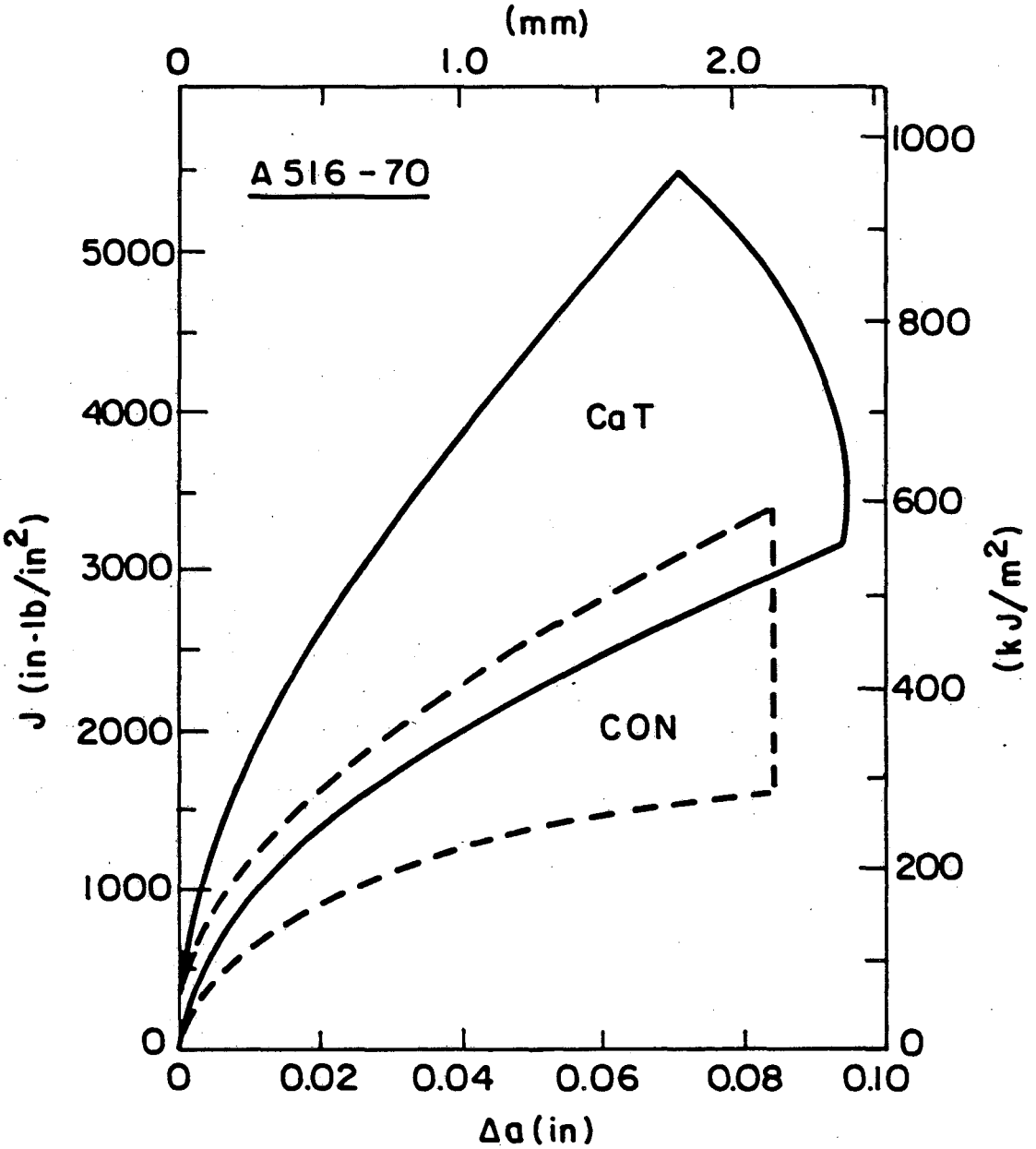

Fig. 2: Experimental data showing $J_R(\Delta a)$ resistance curves for several heats of A516 Grade 70 plain carbon steel plate ($\sigma_o \sim 260$ MPa). Sulphide and oxide non-metallic inclusions have been controlled by both conventional techniques (CON) using vacuum degassing and calcium treatments (CaT). Note how modifying the inclusion distribution has a more significant effect on crack growth compared to crack initiation (from ref. 63).

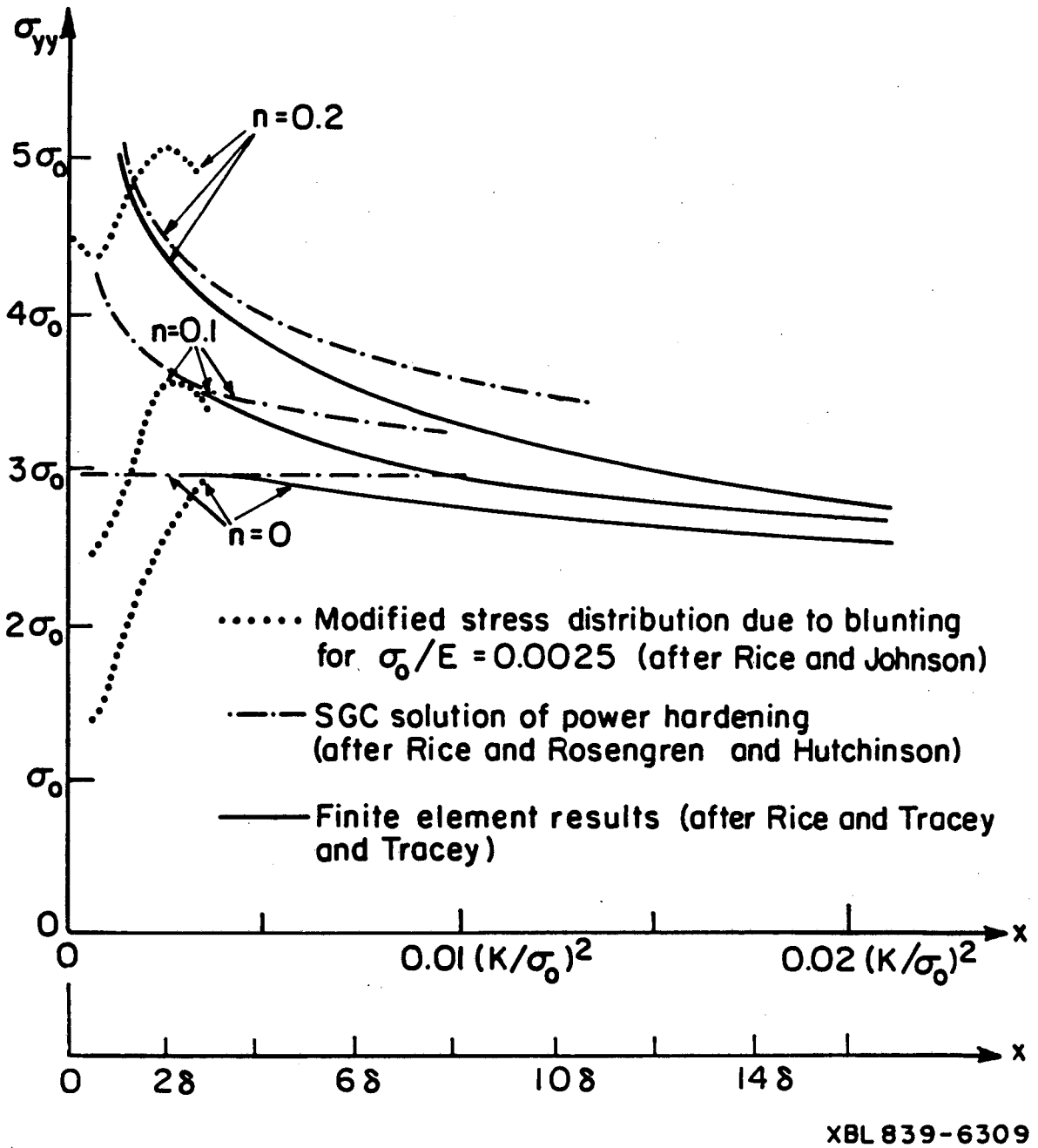

Fig. 3: Distribution of local tensile stress σ_{yy} as a function of distance x directly ahead of a crack tip in plane strain based on HRR small geometry changes (SGC) asymptotic solution for a power hardening solid (from refs. 16 and 17) and the corresponding finite element solutions (from refs. 24 and 37), modified for an initial yield strain σ_0/E of 0.0025 by the finite geometry solution of Rice and Johnson which allows for progressive crack tip blunting (from ref. 22). The abscissa is normalized with respect to both $(K/\sigma_0)^2$ and δ, the CTOD, whereas the ordinate is normalized with respect to the flow stress σ_0.

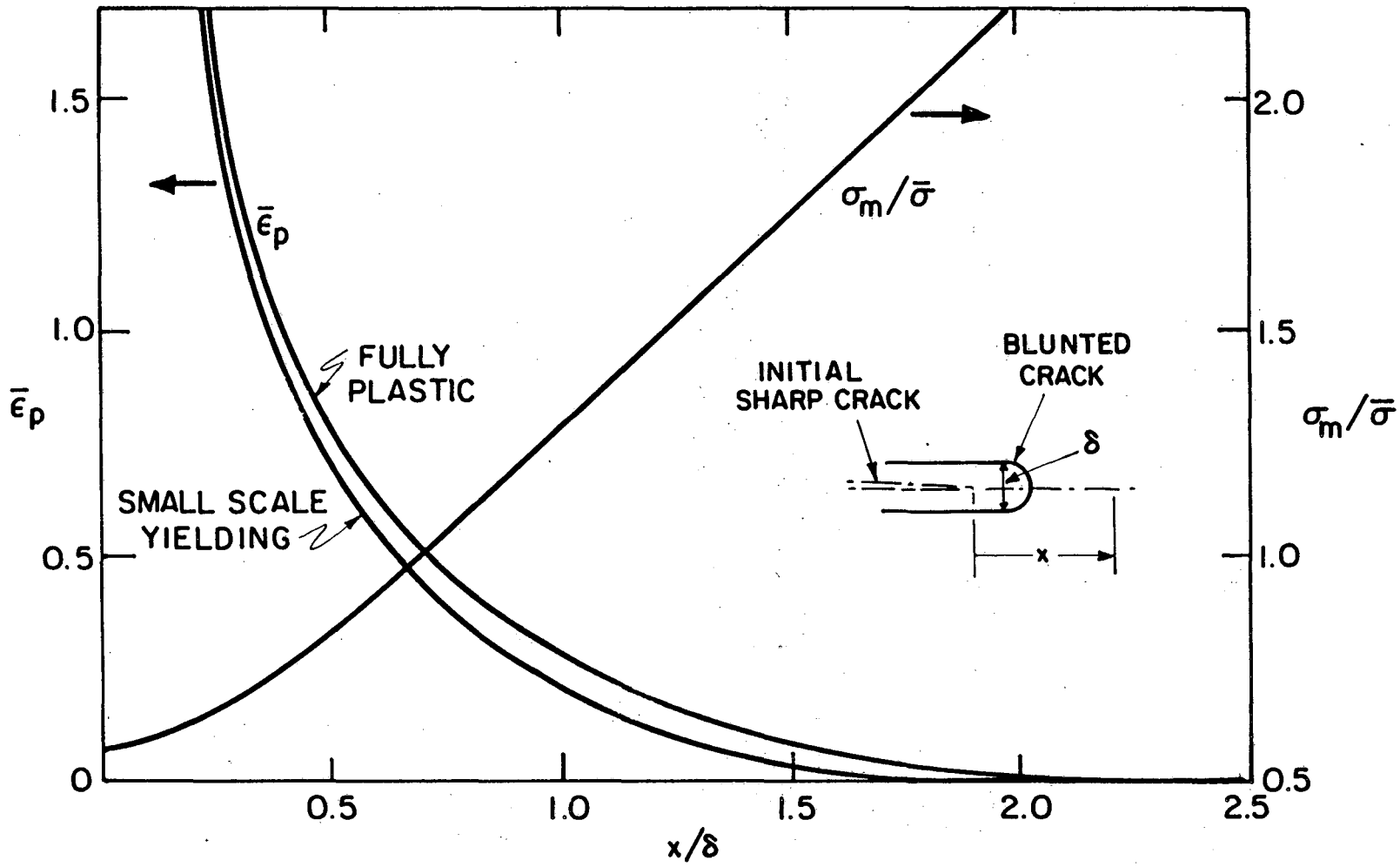

Fig. 4: Distribution of local equivalent plastic strain $\bar{\epsilon}_p$ as a function of distance x, normalized with respect to δ, the CTOD, directly ahead of a crack tip in plane strain, showing the corresponding variation of stress-state ($\sigma_m/\bar{\sigma}$). Solutions based on finite geometry blunting solutions of Rice and Johnson (from ref. 22) and McMeeking (from ref. 23) for both small-scale yielding and fully plastic conditions.

XBL 838-6215

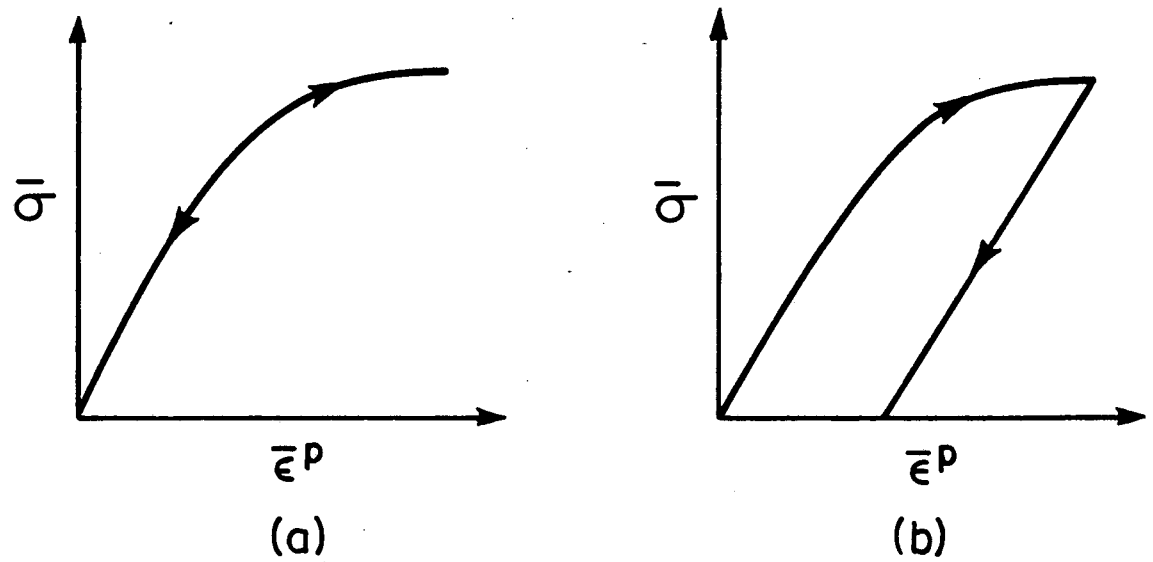

Fig. 5: Idealized constitutive behavior, of equivalent stress $\bar{\sigma}$ as a function of equivalent plastic strain $\bar{\epsilon}_p$, for a) non-linear elastic material conforming to deformation plasticity theory, and b) incrementally-plastic material conforming to flow theory of plasticity.

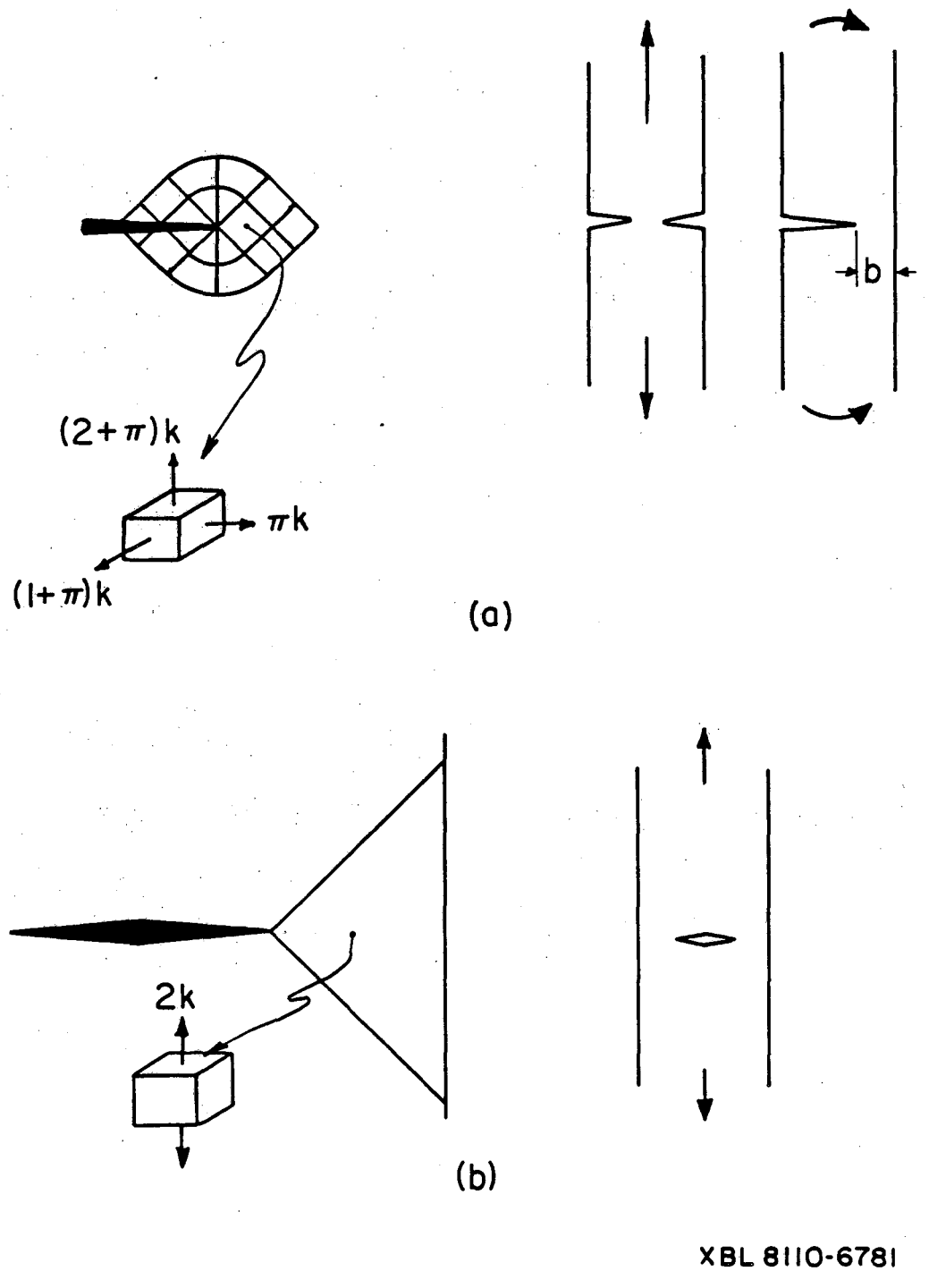

Fig. 6: Fully plastic plane strain slip-line fields for rigid/perfectly plastic solids for a) deep edge-cracked bend and deep double-edge-cracked tension plates (Prandtl field), and b) center-cracked tension plate. k = shear yield stress = $\sigma_o/\sqrt{3}$.

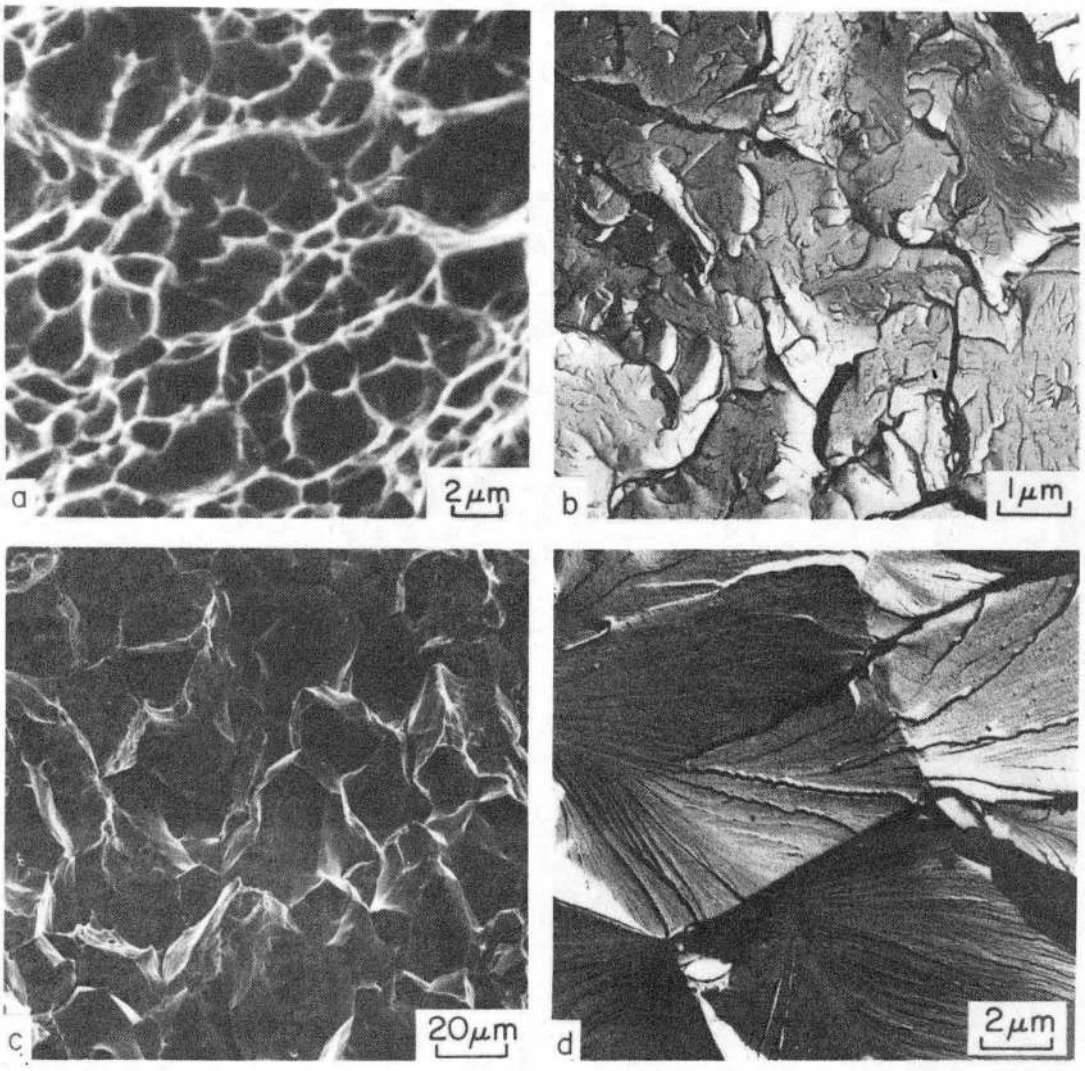

XBB 831-10315

Fig. 7: Classical fracture morphologies showing a) microvoid coalescence, b) quasi-cleavage, c) intergranular cracking and d) transgranular cleavage. Fractographs a) and c) obtained using scanning electron microscopy whereas b) and d) are from transmission electron microscopy replicas.

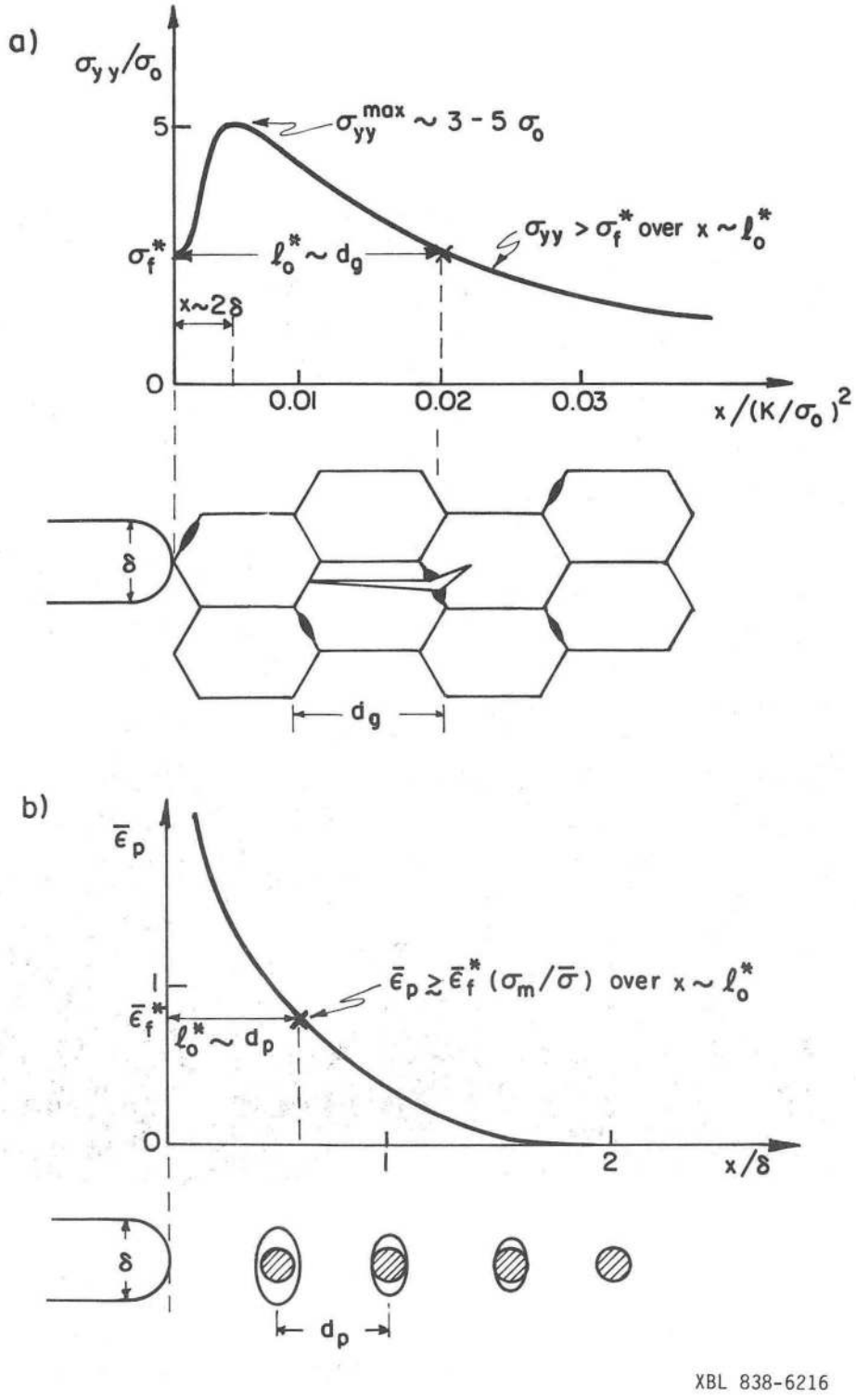

Fig. 8: Schematic idealization of microscopic fracture criteria pertaining to i) critical stress-controlled model for cleavage fracture (RKR) and ii) critical stress-modified critical strain-controlled model for microvoid coalescence.

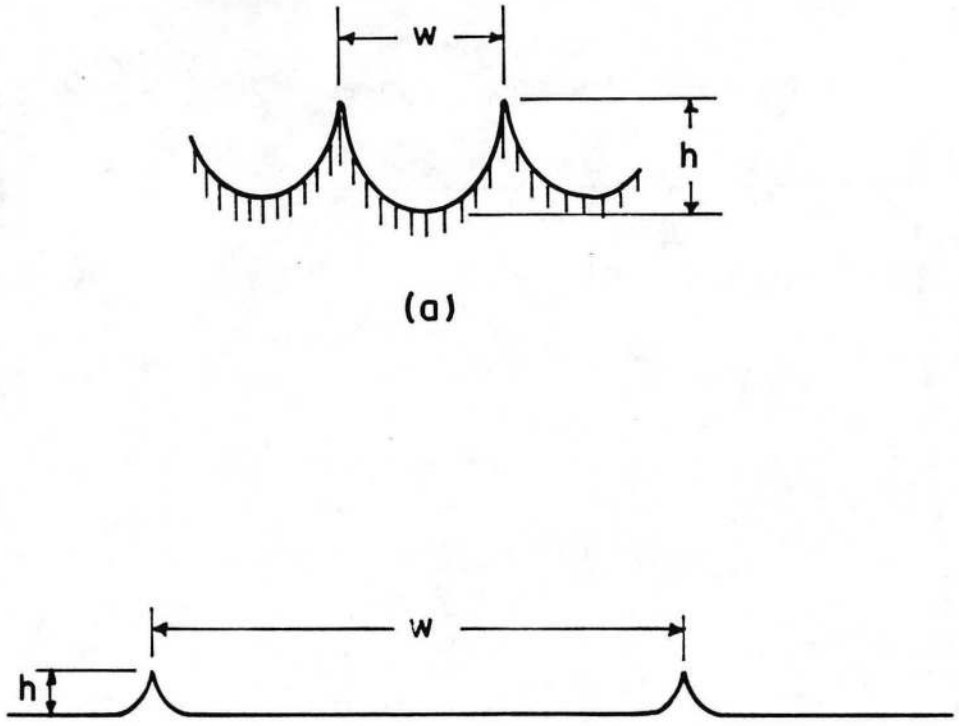

Fig. 9: Definition of fracture surface roughness, M = h/w, for a) microvoid coalescence and b) other locally ductile fracture modes, such as quasi-cleavage.

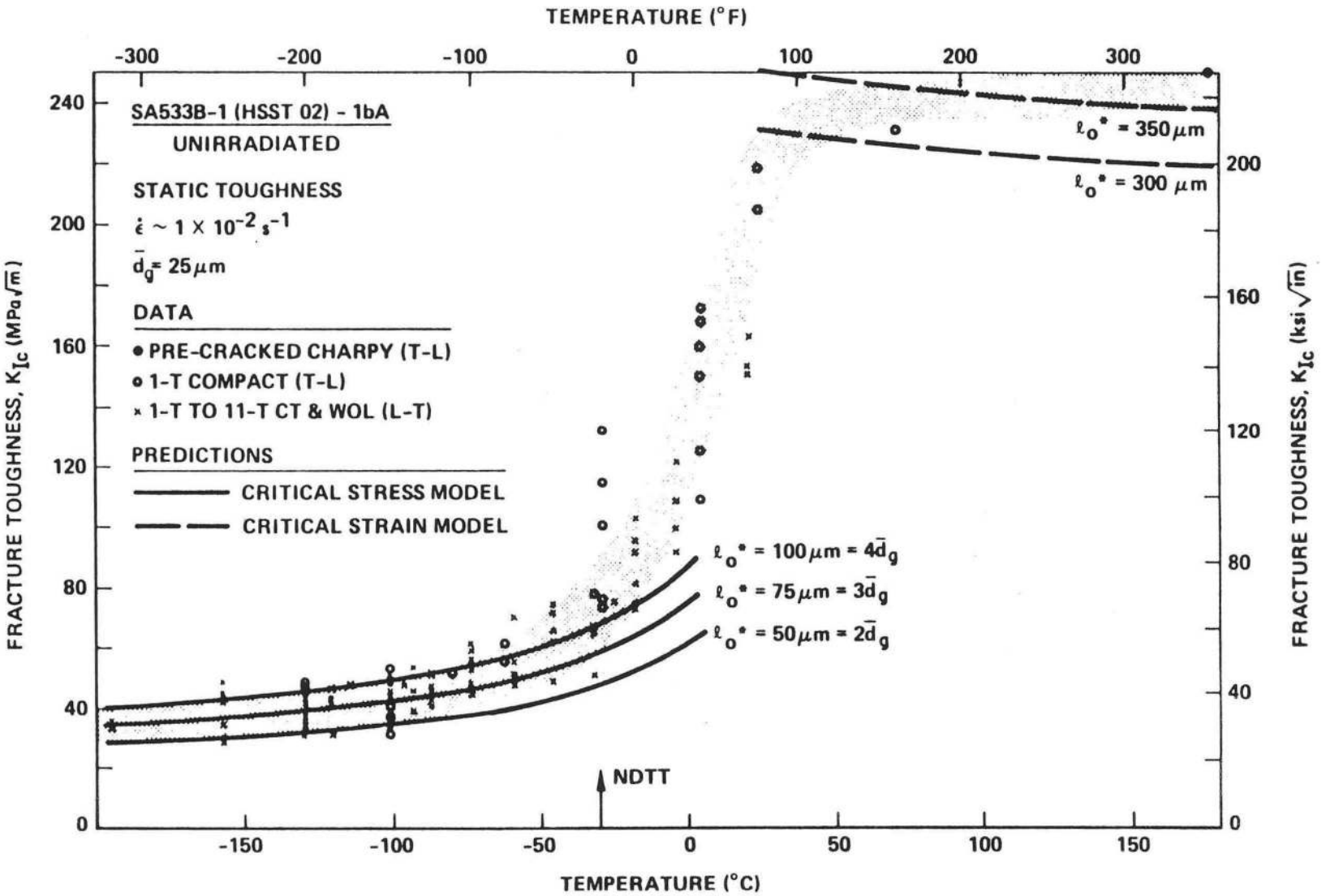

Fig. 10: Comparison of experimentally measured fracture toughness K_{Ic} data for crack initiation in SA533B-1 nuclear pressure vessel steel ($\sigma_0 \sim 500$ MPa) with predicted values based on RKR critical stress model for cleavage on the lower shelf (Eq. 10), and on the stress-modified critical strain model for microvoid coalescence on the upper shelf (Eq. 13), after ref. 29.

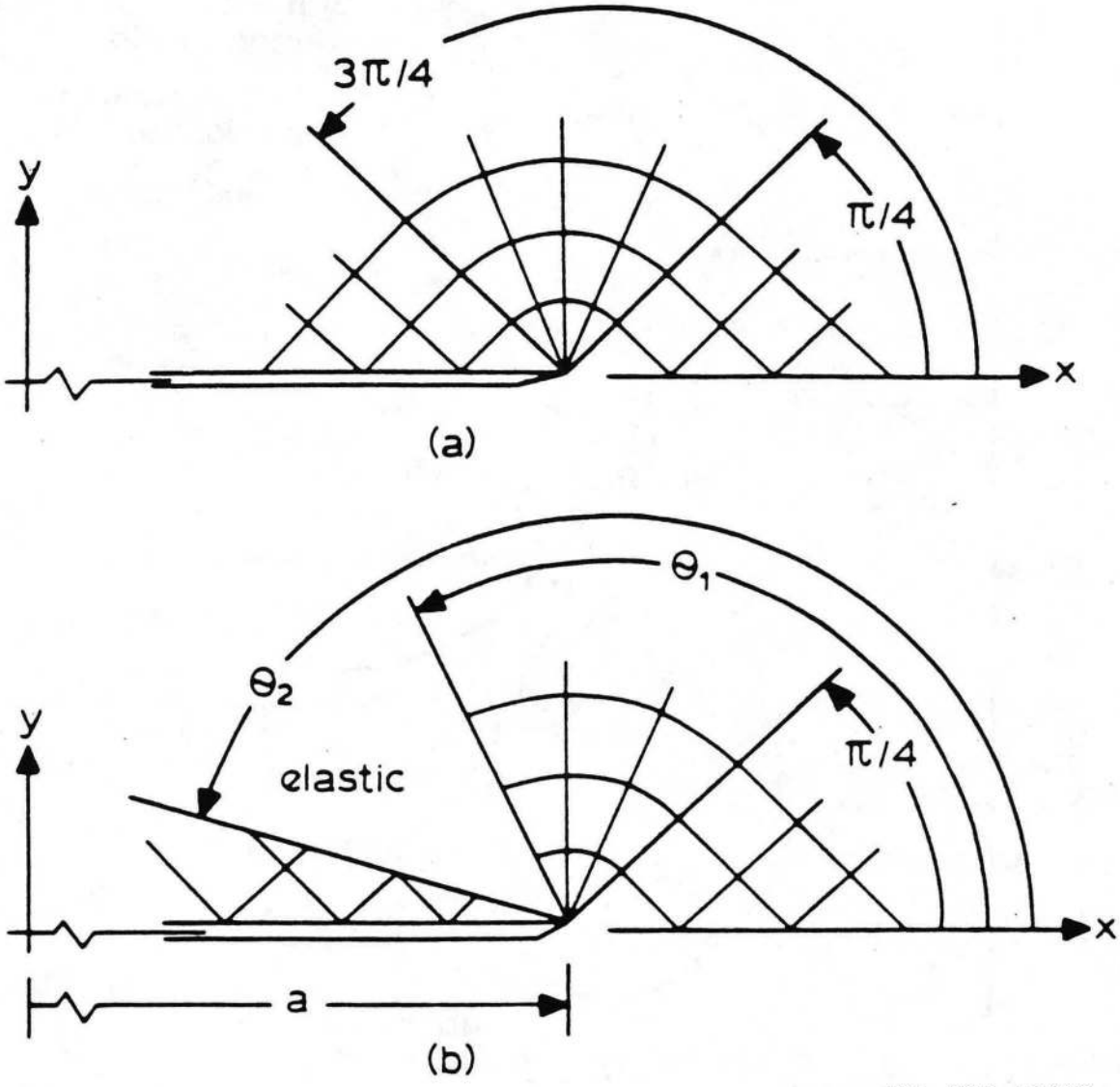

Fig. 11: Plane strain slip-line representation of the crack tip stress-states of the Prandtl field for a) stationary crack, and b) modified with an elastic loading sector behind the tip for a non-stationary crack (after refs. 44 and 48).

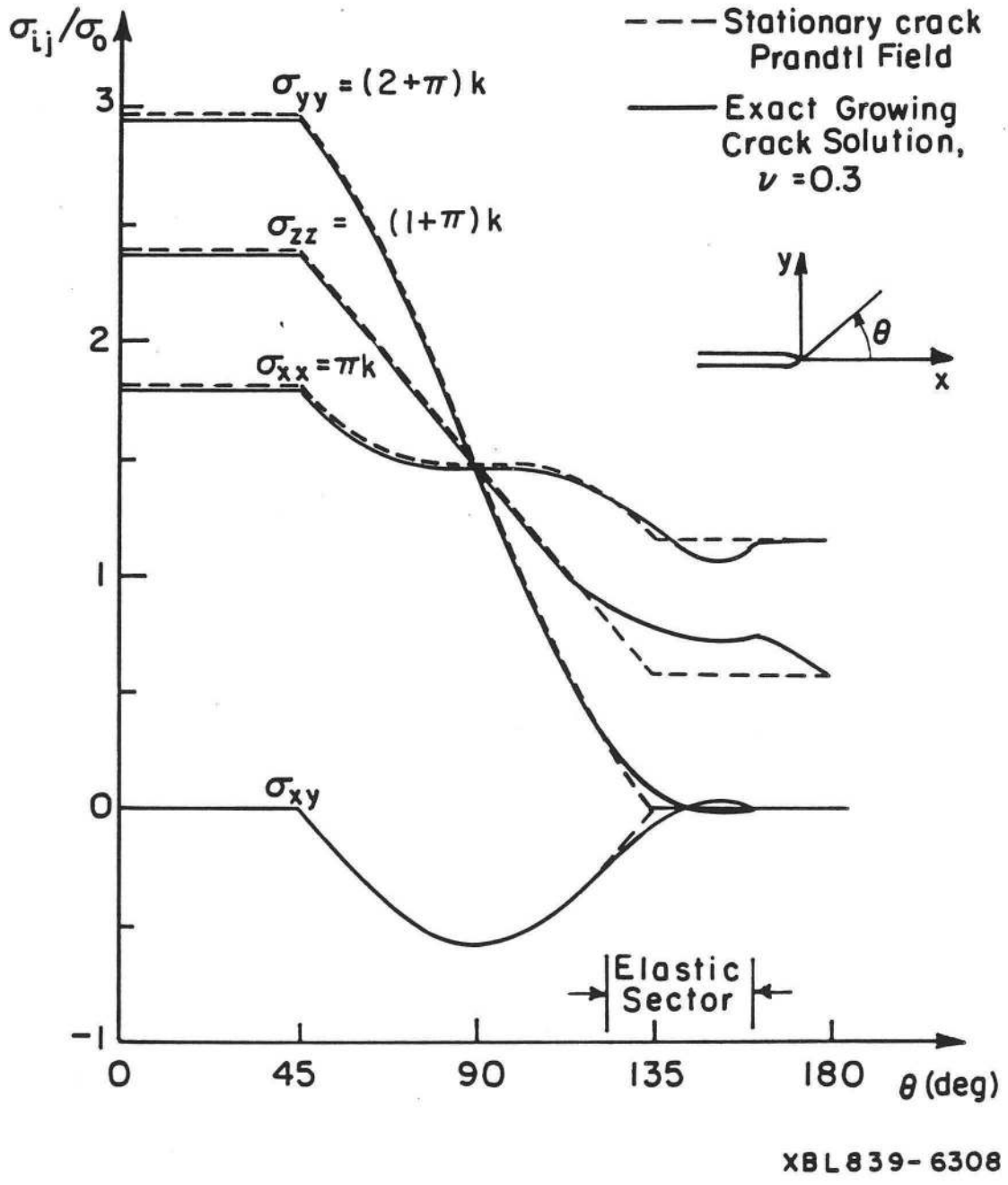

Fig. 12: Comparison of local stresses σ_{ij} ahead of the crack tip in plane strain as a function of angle θ for a) stationary crack based on Prandtl field of Fig. 11a, and b) non-stationary crack based on exact solution for $\nu = 0.3$ of the field shown in Fig. 11b, which contains an elastic unloading sector, after ref. 48. Note how the stress distribution is unchanged by the growing crack, except for $\theta \gtrsim 110^{o}$.

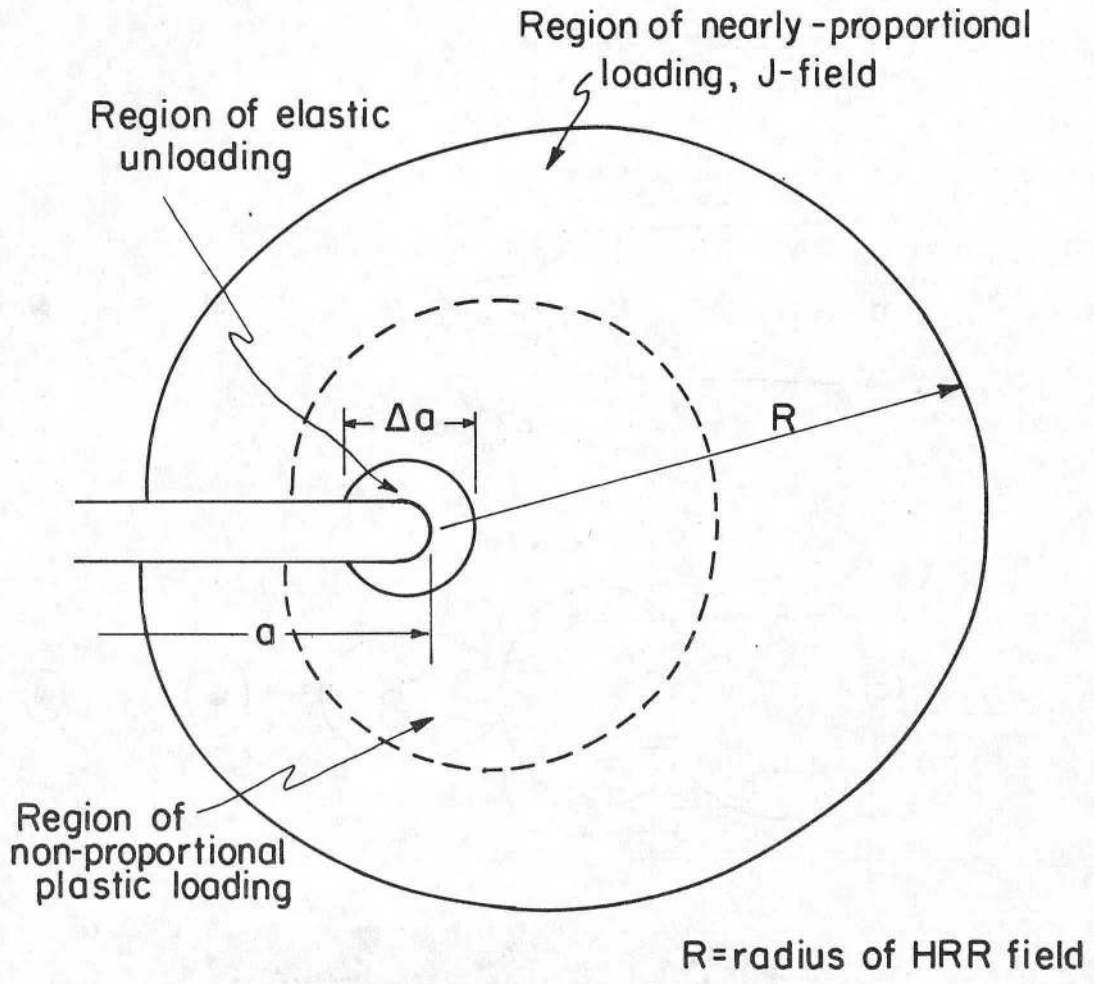

Fig. 13: Schematic representation of the near-tip conditions for a non-stationary crack relevant to the definition of J-controlled growth (after ref. 10).

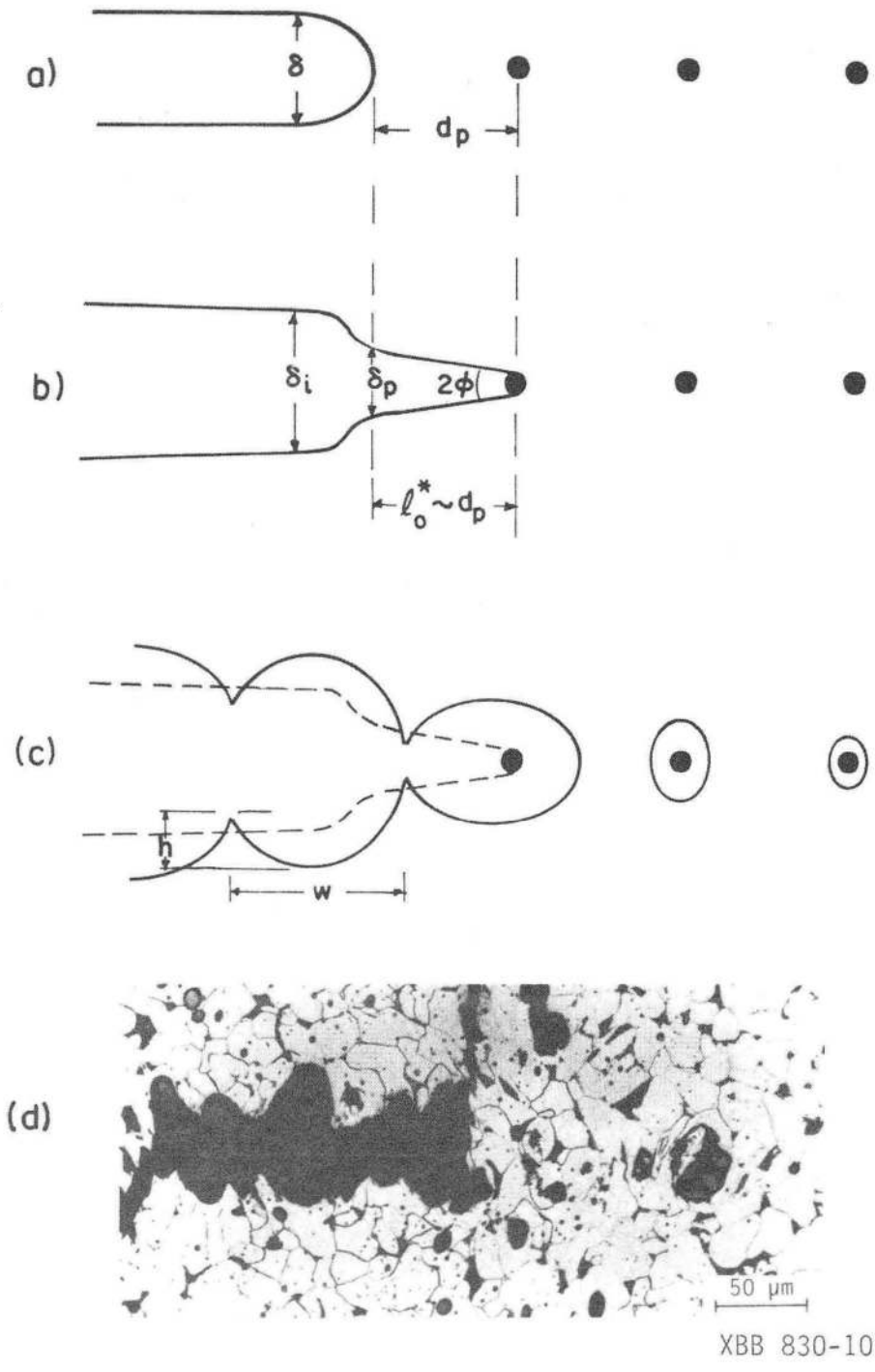

Fig. 14: Idealization of stable crack growth by microvoid coalescence showing a) blunted crack tip, b) crack growth to next inclusion based on constant CTOA (⌀) or on critical CTOD (δ_p) distance ($\ell_o^* \sim d_p$) behind the crack tip, c) morphology of resulting fracture surface relevant to the definition of fracture surface microroughness (M = h/w), and d) fractographic section (after ref. 4) through ductile crack growth via coalescence of voids in free-cutting mild steel.

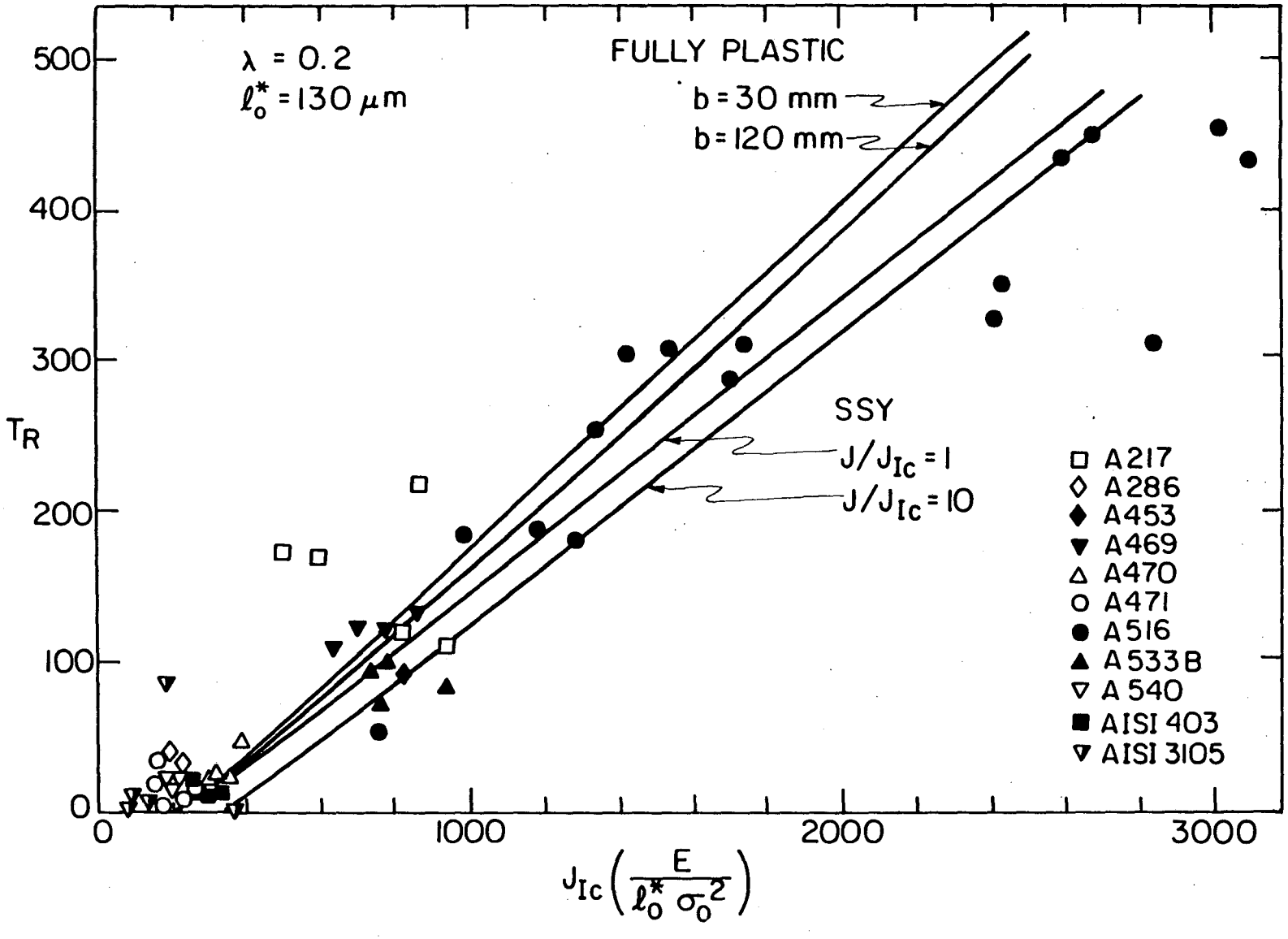

Fig. 15: Variation of crack initiation toughness (J_{Ic}) with crack growth toughness (T_R) showing a comparison of theoretical predictions of Eqs. (49) and (50), for both small-scale yielding (ssy) and fully plastic conditions, with experimental toughness data for steels taken from refs. 7, 63, 67 and 68.

XBL 838-6219

TECHNICAL INFORMATION DEPARTMENT
LAWRENCE BERKELEY LABORATORY
UNIVERSITY OF CALIFORNIA
BERKELEY, CALIFORNIA 94720